Traffic & Transportation

Predicting Operating Speeds of Passenger Cars on Dual–Carriageway Road Tangents

Juraj Leonard VERTLBERG[1], Marijan JAKOVLJEVIĆ[2], Borna ABRAMOVIĆ[3], Marko ŠEVROVIĆ[4]

Original Scientific Paper
Submitted: 28 Sep 2025
Accepted: 30 Oct 2025
Published: 30 Mar 2026

[1] Corresponding author, jvertlberg@fpz.unizg.hr, Faculty of Transport and Traffic Sciences, University of Zagreb, Zagreb, Croatia
[2] mjakovljevic@fpz.unizg.hr, Faculty of Transport and Traffic Sciences, University of Zagreb, Zagreb, Croatia
[3] babramovic@fpz.unizg.hr, Faculty of Transport and Traffic Sciences, University of Zagreb, Zagreb, Croatia
[4] msevrovic@fpz.unizg.hr, Faculty of Transport and Traffic Sciences, University of Zagreb, Zagreb, Croatia

Publisher:
Faculty of Transport and Traffic Sciences, University of Zagreb

ABSTRACT
This research develops multiple linear regression models for predicting operating speeds (V85) of passenger cars on dual–carriageway road tangents in Croatia, separately for the right (driving) and left (overtaking) lanes. Thirty-nine locations were analysed, with 26 locations used for model development and 13 for validation. Operating speeds were measured with a drone under free–flow conditions, ensuring consistency and accuracy of observations. Following a correlation analysis, ANOVA testing and multicollinearity diagnostics, stepwise regression was applied to identify statistically significant predictors from 14 infrastructural, traffic and environmental variables. The final models include factors such as total tunnel length, speed limit, lane width, longitudinal slope, average summer daily traffic (ASDT) and traffic flow density, with results differing between lanes. The right (driving) lane model achieved an explanatory power of $R^2 = 0.82$ (RMSE = 4.85), while the left (overtaking) lane model achieved $R^2 = 0.71$ (RMSE = 6.36). Validation on test locations confirmed the models' predictive capability, with an average absolute deviation of 5.16% for the right lane and 4.75% for the left lane. The results provide practical approaches for evaluating the consistency of road designs, managing vehicle speeds and assessing safety, while laying the groundwork for future improvements to lane–specific prediction models.

KEYWORDS
operating speed; V85; road safety; road tangents; traffic accidents; dual–carriageway roads; prediction model.

1. INTRODUCTION

The regulation and understanding of vehicle speed remain among the most critical challenges in improving road safety worldwide. Speed is consistently identified as a leading contributing factor in road traffic accidents, directly influencing both their occurrence and the severity of consequences. Based on the data from the World Health Organisation, road traffic accidents claim over 1.19 million lives each year and represent the primary cause of death among individuals aged 5–29 years [1]. A substantial share of these fatalities, often estimated at roughly one-third, is linked to speeding or inappropriate speed selection [2, 3]. Similar findings are echoed by European and Australian studies, which attribute around 30–40% of fatal accidents to excessive or inappropriate speed [4, 5]. In Croatia, data indicate that speed contributed to 39% of serious road traffic accidents, and in about 17% of cases, it was the primary causal factor [6]. These figures reinforce the understanding that speed management is not merely a question of compliance with posted speed limits but a fundamental component of sustainable road safety policy.

Within the traffic and road safety engineering domain, the operating speed, commonly defined as the 85th percentile speed under free-flow traffic conditions, occupies a unique role. Unlike the design speed, which is determined during the planning phase, or the posted speed limit, which is a regulatory measure, operating speed reflects the real-world behaviour of drivers. In free-flow traffic conditions, when drivers are unconstrained by congestion or enforcement, operating speed represents the speed most drivers "choose" to drive. This behavioural speed often diverges from the speed limit, particularly on high-quality roads where drivers perceive higher speeds as safe. Studies across Europe reveal that 35% and 75% of observed vehicle speeds exceed statutory limits [7], underscoring the limitations of relying solely on speed limits to influence driver behaviour. In addition to roadway geometry and traffic conditions, vehicle-road interactions, especially tyre performance and inflation pressure, play a direct role in vehicle control, lateral stability and braking performance, and therefore influence the speeds drivers choose as safe. Numerical simulation and experimental tyre studies have shown that load and inflation variations change the tyre contact dynamics and braking margins in ways that could alter safe operating speeds under free-flow conditions [8]. Including this vehicle-level mechanism connects infrastructure and traffic predictors with vehicle capability, broadening the theoretical background and linking speed models to the wider domain of vehicle dynamics and road safety research [9].

The ability to predict operating speed is therefore critical for road designers and safety analysts. Operating speeds can be measured directly on existing roads, but they can only be predicted on newly designed or significantly reconstructed roads. Accurate predictions enable the design of roads that inherently promote safe speeds and help align design speed, operating speed and speed limits, an alignment research has shown to be a cornerstone of design consistency and road traffic accident risk reduction [10, 11]. When operating speed significantly exceeds the design speed or speed limit, drivers may encounter unexpected situations, misjudge stopping distances or be less able to respond safely to hazards, all of which raise the likelihood of road traffic accidents and therefore amplify their consequences [12].

Over the past decades, researchers have developed numerous models linking road infrastructure, traffic and environmental factors to operating speed. These models have traditionally been statistical, employing linear regression or similar methods, though in recent years, more experimental approaches based on artificial intelligence (e.g. neural networks, support vector machines) have appeared [13–17]. Regardless of the method, most operating speed prediction research shares two characteristics: it focuses on extra-urban, single-carriageway roads and emphasises horizontal curves (and a combination of horizontal curves and tangents) [18–25]. Despite being the segments where the highest speeds are typically reached and maintained, road tangents have been studied less intensively, and the literature on dual-carriageway roads is notably thinner. Even when dual-carriageway sections are included, they are often treated as homogeneous facilities, without considering that driver behaviour and speed selection differ substantially between the right (driving) lane and the left (overtaking) lane [26, 27]. This gap is critical, as dual-carriageway roads, which usually carry the largest volumes of traffic, are designed for higher speeds, and are perceived by drivers as "safer", often leading to greater speeds [30]. The differences between lanes further complicate the picture: the left lane is typically used for overtaking and faster drivers, while the right lane accommodates more diverse vehicle types, including heavy goods vehicles, and reflects a broader range of speed choices. Developing lane-specific operating speed prediction models for these roads is essential, both for supporting infrastructure design decisions and informing targeted safety interventions, such as speed harmonisation strategies or enforcement prioritisation.

This research builds on a structured program addressing operating speed on road tangents. In earlier research, the relationship between operating speed and a wide range of infrastructural, traffic and environmental variables was examined separately for single- and dual-carriageway road tangents, establishing a foundational understanding of the factors influencing operating speed but without developing predictive models [31]. A subsequent study concentrated on single-carriageway road tangents, resulting in the development and validation of an operating speed prediction model for passenger cars [32]. This research represents the third stage in this trajectory and addresses the remaining knowledge gap by focusing on dual-carriageway road tangents.

The primary objective of this study is to develop and validate an operating speed prediction model for passenger cars on dual-carriageway road tangents, distinguishing between the right (driving) and left (overtaking) lanes. An enhanced dataset was analysed to achieve this, originally compiled for prior research [31] and expanded with additional locations and measurements. Separate models were developed for each lane, reflecting the differing speed dynamics. The research identifies the key infrastructural, traffic and

environmental variables that influence operating speed on dual-carriageway road tangents and provides tools for predicting operating speeds without field measurements and, more importantly, in the design phases.

By addressing the lane-level prediction of operating speed on dual-carriageway road tangents, this study contributes to both the academic literature and practical road design. It provides evidence-based insights that can be used to improve design consistency, align speed expectations with road function, and ultimately support the goal of reducing road traffic accidents and mitigating their severity.

2. METHODOLOGY

Figure 1 concisely illustrates the methodology, while the subsequent subsections elaborate on each phase in detail.

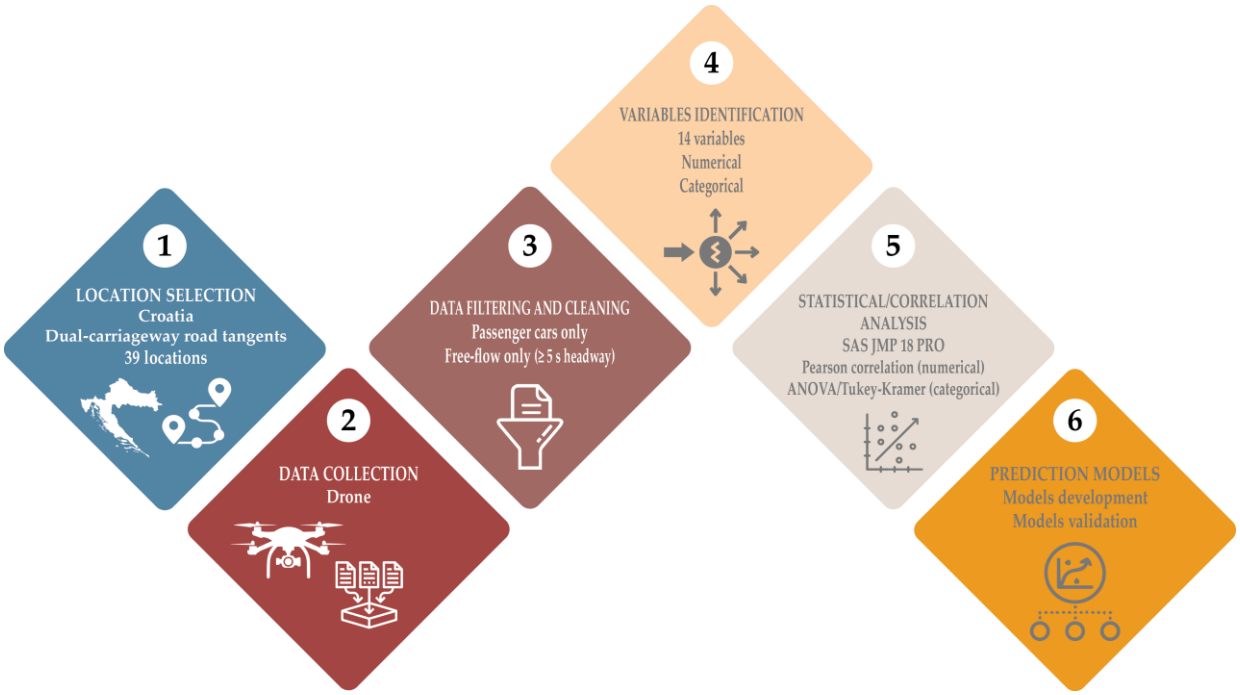

Figure 1 – Workflow diagram of the applied methodology

2.1 Data collection

The empirical foundation of this research rests on an expanded dataset of operating speeds (V85) collected on dual–carriageway roads (motorways) tangents in Croatia. Compared to earlier research, which initially covered 10 cross–sections (20 locations) on motorways [31], this research enlarges the sample with an additional 19 locations obtained through newly conducted surveys, thus providing a more comprehensive representation of speed behaviour. The selection of locations was undertaken to ensure geographical, infrastructural and traffic representativeness while excluding locations where external influences, such as road works or atypical traffic patterns, could bias results. Therefore, operating speeds were measured in only one direction at several motorway cross sections, as the opposite carriageway exhibited temporary irregularities that could bias results. Such abnormalities included roadworks, stalled or broken–down vehicles or atypical traffic management measures that could distort free–flow operating speeds (V85). By carefully excluding these carriageways and supplementing the dataset with additional, unaffected locations, the analysis ensured that the final sample reflected genuine, unconstrained speed sample and preserved the methodological consistency required for model development.

Representative measurement locations were distributed on the motorway network across Croatia (*Figure 2*). The selection criteria accounted for variations in posted speed limits (100, 110, 120 and 130 km/h), traffic volumes (expressed through average annual daily traffic – AADT and average summer daily traffic – ASDT), and terrain type (flat, hilly and mountainous), thereby capturing a broad spectrum of road, traffic and environmental conditions. To guarantee methodological consistency, each measurement location was positioned away from horizontal and vertical curves, junctions, toll stations or construction zones that could distort natural speed patterns. Additionally, only extra–urban areas were considered to avoid the confounding effects of local access.

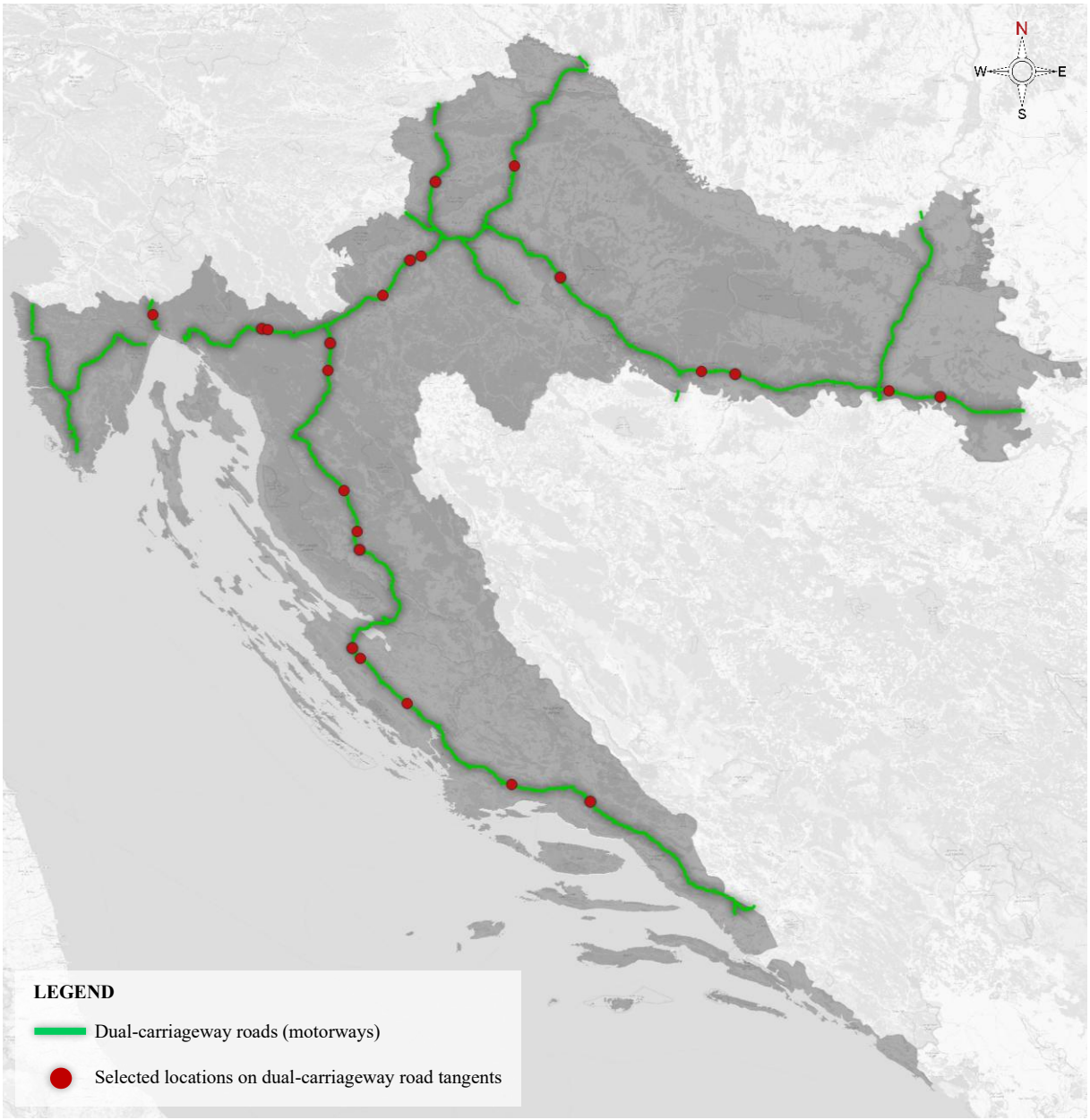

Figure 2 – Location map of the surveyed dual–carriageway tangents in Croatia [31]

Operating speed data were obtained using unmanned aerial vehicle (UAVs)–drone, following a validated drone–based methodology [31]. Aerial recordings were conducted during good weather conditions (good visibility, moderate temperatures and the absence of precipitation or strong winds) to ensure uninterrupted flights and reliable video quality. UAV flights were scheduled during off–peak weekday periods to minimise the influence of congestion and to capture free–flow conditions. For each selected cross–section, two detection lines were defined along a tangent segment approximately 100 m long. Vehicle passage times at the entry and exit lines were manually extracted from high–resolution video footage and processed to calculate vehicle speeds. The spatial and temporal accuracy of UAV-derived trajectories has been shown to exceed that of conventional roadside sensors. Previous validations indicate that UAV measurements typically achieve position errors below 0.2 m and speed errors under 1 km/h, which is notably higher precision than single-point radar or loop detector systems that are limited by fixed detection zones and sampling intervals [32]. This enhanced accuracy allows for continuous, lane-level observation of vehicle dynamics across the full road segment. It should be emphasised that the same drone–based procedure, as previously applied in the earlier research [31], was employed for the additional locations, thereby ensuring methodological consistency across the expanded dataset. This procedure was carried out separately for the right (driving) and left (overtaking) lanes, enabling the development of distinct prediction models for each lane.

In this research, the dependent variable is the operating speed (V85) of passenger cars, computed separately for the right (driving) and left (overtaking) lanes under free–flow conditions (time gap between vehicles ≥ 5 s). While speeds of non–passenger vehicles were not used to form the response, all passing vehicles were classified during video annotation so that traffic composition and demand indicators, most notably the heavy goods vehicle (HGV) share, including buses, could be derived as candidate predictors. Consistent with the procedure in the earlier research [31], HGV share was obtained from the drone–based vehicle classification by lane, whereas AADT and ASDT were taken from official counts and, for carriageways, apportioned equally to each carriageway when only cross–section totals were available. This preserves methodological continuity while focusing the model on passenger–car operating speeds.

A total of 20,878 vehicle observations were collected in this study (Appendix A). The dataset was then subjected to a structured preprocessing workflow designed to remove anomalies and extreme outliers, ensuring the reliability of subsequent analyses. Initially, each variable (including speed measurements) was visually inspected to identify inconsistent records that fell outside expected engineering and physical ranges. Entries confirmed as erroneous based on original field documentation were corrected; otherwise, they were excluded from the dataset. To maintain comparability, only passenger cars were included in the analysis. Motorcycles were omitted due to their minimal presence in the traffic flow, which would have yielded a statistically unreliable sample. Similarly, heavy goods vehicles and buses were excluded because they follow lower speed regulations and often use tachographs, affecting speed patterns. The analysis was further restricted to off–peak traffic periods to minimise the influence of congestion on driving behaviour. Additionally, a minimum time gap of five seconds between consecutive vehicles was enforced to ensure that only free–flow operating speeds were captured. After these filtering steps, 4,743 valid observations remained, with 2,693 from the right (driving) lane and 2,050 from the left (overtaking) lane.

This approach established a new and enlarged database of operating speeds of passenger cars on dual–carriageway road tangents. The dataset provides the empirical basis for analysing the influence of infrastructural, traffic and environmental variables and for developing lane–specific operating speed prediction models.

2.2 Variables identification

For the purpose of developing operating speed prediction models on dual–carriageway road tangents, a set of 14 explanatory variables was identified. These variables encompass infrastructural, traffic and environmental elements that may influence passenger cars' operating speeds (V85). The selection process was based on insights from the earlier studies on both single carriageway and road tangents [31, 33], complemented by the specific features of the newly collected dataset. Each variable was examined for its theoretical relevance and potential explanatory power concerning lane–specific speed behaviour, emphasising distinguishing between the right (driving) and left (overtaking) lanes.

The final list of variables is as follows:

— Heavy goods vehicle share (right lane, left lane): The percentage of heavy goods vehicles and buses in the traffic flow is recorded separately for each lane. This variable captures the influence of slower and larger vehicles on passenger cars' operating speeds.
— Total tunnel length in the last 20 km: The cumulative length of motorway tunnels within the 20 km preceding the measurement location. Tunnels represent constrained environments that may affect driver behaviour beyond their immediate locations, particularly regarding speed adaptation and perception of alignment continuity.
— Speed limit: The regulatory speed limit (100, 110, 120 or 130 km/h), obtained from field surveys. This variable reflects the primary legal framework for driver speed choice and serves as a benchmark for analysing deviations in actual operating speeds.
— Lane width: The measured width of road lanes at each location, expressed in metres.
— Design speed (Vp): As defined by Croatian road design standards, it represents the highest speed at which complete driving safety is guaranteed in free–flow traffic conditions along the entire section of a road, under optimal weather conditions and with proper road maintenance [34].
— Previous object distance: The longitudinal distance between the measurement point and the last nearest infrastructure facility (e.g. bridge, junction).
— Following object distance: The longitudinal distance from the measurement point to the next infrastructure facility. Both the following object distance and the previous object distance were derived from GIS and Google Earth imagery. The locations of preceding and following vehicles were identified from orthophotos

and lane geometry, and their distances were computed along the lane centreline at corresponding timestamps. The imagery and UAV video were cross-checked to ensure consistency, and positional accuracy was considered sufficient for free-flow speed modelling.

— Longitudinal slope: The slope of the road section at the measurement site.
— Terrain type: A categorical variable (flat, hilly, mountainous) describing the broader topographic setting of the road. Terrain type influences alignment design (e.g. frequency of curves, slope intensity) and driver expectations, potentially shaping speed behaviour.
— AADT: The annual daily traffic and traffic volumes obtained from official datasets. Since data were only available for the combined cross–section, individual carriageway values were approximated by dividing the total by two.
— ASDT: The average daily summer traffic and traffic volumes obtained from official datasets. Since data were only available for the combined cross–section, individual carriageway values were approximated by dividing the total by two.
— Traffic flow density (right lane, left lane): Lane–specific density values derived from traffic flow observations are expressed in the number of vehicles per kilometre per lane.

The identified variables jointly provide a comprehensive description of infrastructural, traffic and environmental elements potentially influencing operating speeds on dual–carriageway road tangents. Their inclusion ensures that the developed prediction models account for physical road attributes and dynamic traffic flow parameters while differentiating between the right (driving) and left (overtaking) lanes.

2.3 Data analysis

The analytical procedure in this research was carried out using SAS JMP Pro 18 and followed a structured sequence designed to ensure both statistical representativeness and interpretability of the results. The first step involved preprocessing of the dataset, which consisted of operating speed (V85) observations collected at 39 tangent locations. To guarantee data quality, each observation was carefully screened for potential errors in video annotation and speed computation. Only passenger–car speeds under free–flow conditions (time headways ≥ 5 s) were retained, ensuring that the dependent variable reflected unconstrained speed behaviour. Extreme or atypical values attributable to temporary influences, such as roadworks and traffic incidents, were identified and excluded from further analysis. This filtering resulted in a dataset reliably representing typical operating conditions on dual–carriageway road tangents.

After preparing the data, the study systematically explored the statistical relationships between operating speed and the selected explanatory variables. For continuous variables, normality was evaluated using the Shapiro–Wilk test. Variables that met the normality assumption were examined with Pearson correlation coefficients, whereas variables that did not were analysed using Spearman's rank–order correlation. This approach enabled the assessment of both linear and monotonic associations. A significance threshold of $\alpha=0.05$ was applied in determining statistically relevant associations. For variables such as terrain type or speed limit that are analysed as both categorical and (for the model development purpose) continuous, one–way ANOVA test was used to compare operating speed across categories. Where statistically significant differences were observed, the Tukey–Kramer post hoc procedure was applied to identify and quantify pairwise differences. To prepare these categorical predictors for regression modelling, they were subsequently transformed into continuous or dummy variables, thereby preserving their explanatory role while ensuring compatibility with the requirements of multiple linear regression.

Due to operating speed being influenced by interdependent infrastructural, traffic and environmental factors, particular care was given to diagnosing multicollinearity. A correlation matrix was constructed to evaluate the degree of overlap between candidate predictors. In cases where strong correlations were observed, the variable with weaker theoretical justification or explanatory power was excluded. For example, the high correlation between AADT and ASDT required the retention of only one traffic exposure measure, while the conceptual proximity of lane width and design speed was handled similarly. Variance inflation factors (VIFs) were also calculated for all retained predictors, with all values remaining below the conservative threshold of 5, verifying that no problematic multicollinearity exists and ensuring the reliability of coefficient estimates.

Model development was conducted using multiple linear regression, chosen for its interpretability and ability to quantify the explicit contribution of each explanatory variable to operating speed. A stepwise forward selection approach was employed, beginning with the most statistically significant predictors and progressively adding variables that improved the explanatory capacity of the model while aiming for the 95% confidence

level requirement. This ensured that the final specification remained parsimonious while capturing the key determinants of operating speed behaviour. The general mathematical form of the models is expressed as:

$$Y = a\_0 + \sum b\_i \; X\_i \tag{1}$$

where Y = dependent variable, a_0 = regression constant, b_i = regression coefficient and X_i = explanatory variables.

The diagnostic phase included an examination of standardised and studentised residuals, leverage values and Cook's distance. Model assumptions were further verified through residual analysis. Histograms, Q–Q plots and scatterplots of residuals against fitted values were examined to confirm normality and linearity. The residuals were also tested for normality using the Shapiro–Wilk method, to confirm that the normality assumption could not be rejected.

Finally, validation of predictive performance was conducted using an external test dataset consisting of 13 locations (≈1/3 of the total sample) that were not used during model development. At each location, the observed V85 was compared with the value predicted by the model, and prediction errors were evaluated using absolute differences [km/h] and relative deviations [%].

3. RESULTS AND DISCUSSION

3.1 Analysis of the relationship between operating speed and selected explanatory variables

This section examines the relationship between operating speed (V85) and various variables on dual–carriageway road tangents, based on the training dataset comprising 26 locations. The analytical techniques were chosen according to the characteristics of each variable type, as summarised in *Table 1*.

Table 1 – Statistical methodology for identifying variables using the training dataset (26 locations)

Variables (dual–carriageway road tangents)	Variable type	Normal distribution	Test used
Total tunnel length in the last 20 km	Continuous	NO	Spearman
Speed limit	Categorical/Multi–level	—	ANOVA
Lane width	Categorical/Multi–level	—	ANOVA
Design speed	Categorical/Multi–level	—	ANOVA
Previous object distance	Continuous	NO	Spearman
Following object distance	Continuous	NO	Spearman
Longitudinal slope	Continuous	YES	Pearson
Terrain type	Categorical/Multi–level	—	ANOVA
Heavy goods vehicles share (left lane)	Continuous	NO	Spearman
Heavy goods vehicles share (right lane)	Continuous	YES	Pearson
AADT	Continuous	NO	Spearman
ASDT	Continuous	YES	Pearson
Traffic flow density (left lane)	Continuous	NO	Spearman
Traffic flow density (right lane)	Continuous	NO	Spearman

The Shapiro–Wilk test was initially applied for continuous variables to evaluate whether the data conformed to a normal distribution. This assessment was necessary to verify the validity of the normality assumption. Variables that satisfied this assumption were examined using Pearson correlation, whereas those that did not were analysed with Spearman's rank–order correlation. The complete results of the normality assessment (Shapiro–Wilk test) are presented in *Figure 3*.

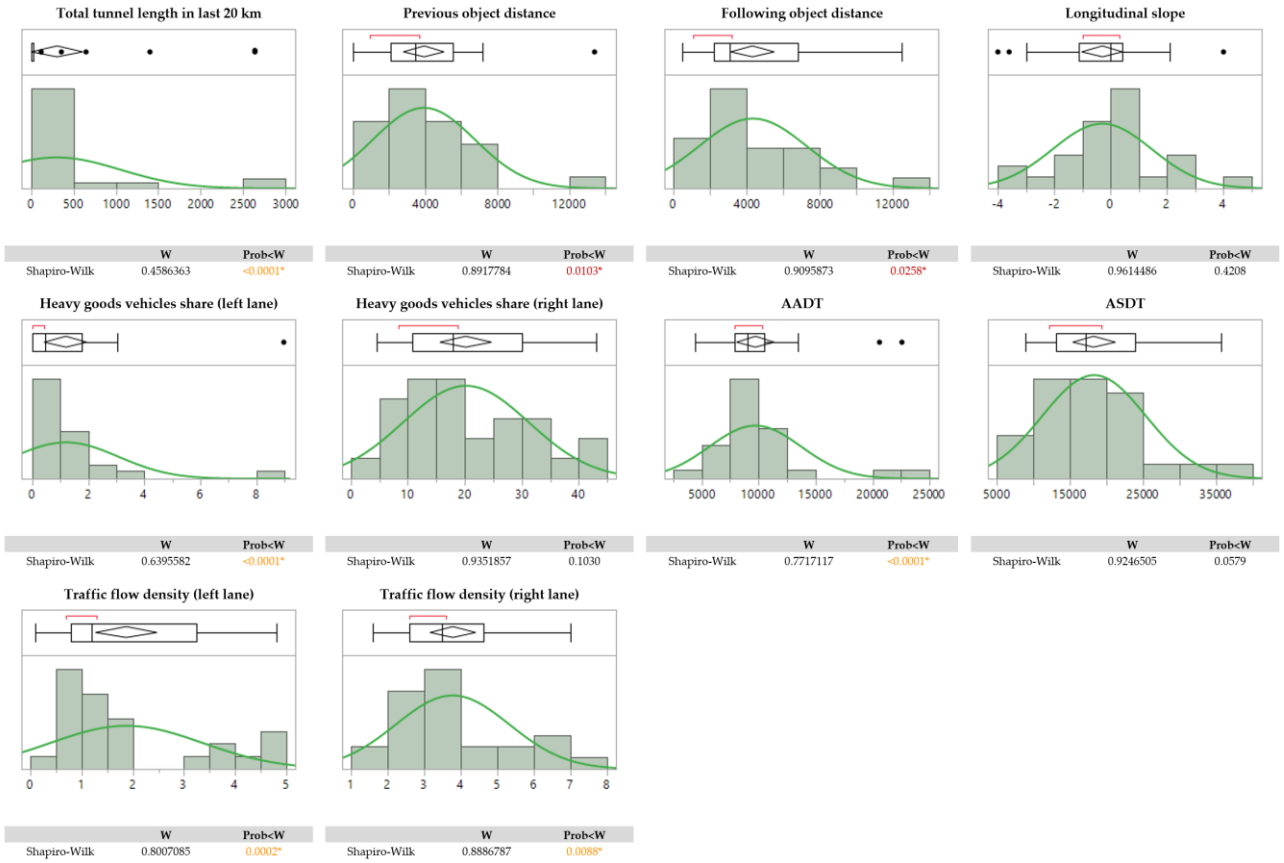

Figure 3 – Assessment of normality using the Shapiro–Wilk test

Further analysis of the relationship between operating speed (V85) and the identified explanatory variables was conducted separately for the right (driving) and left (overtaking) lanes. This distinction was required due to the functional and behavioural differences between the two lanes. The right lane accommodates a more heterogeneous traffic flow, including a higher share of heavy vehicles, which typically results in lower and more dispersed operating speeds. Conversely, the left lane is predominantly used for overtaking manoeuvres by passenger cars, where higher and more homogeneous operating speeds are observed.

A Tukey–Kramer test was conducted to statistically confirm these differences and compare the mean operating speeds between lanes (*Figure 4*). The results showed that the mean V85 in the left lane was 159.71 km/h, while it was 144.72 km/h in the right lane. The 14.99 km/h difference was highly significant ($p < 0.0001$), with a 95% confidence interval ranging from 10.90 to 19.08 km/h. These results demonstrate that the mean operating speeds of passenger cars differ significantly between the two lanes, justifying the need for separate analyses. Indeed, the observed difference between left- and right-lane operating speeds can also be attributed to variations in vehicle type distribution. The right lane is more frequently occupied by heavy goods vehicles and slower traffic, while the left lane is predominantly used by passenger cars performing overtaking manoeuvres, which typically results in higher operating speeds under comparable geometric and traffic flow conditions [35, 36].

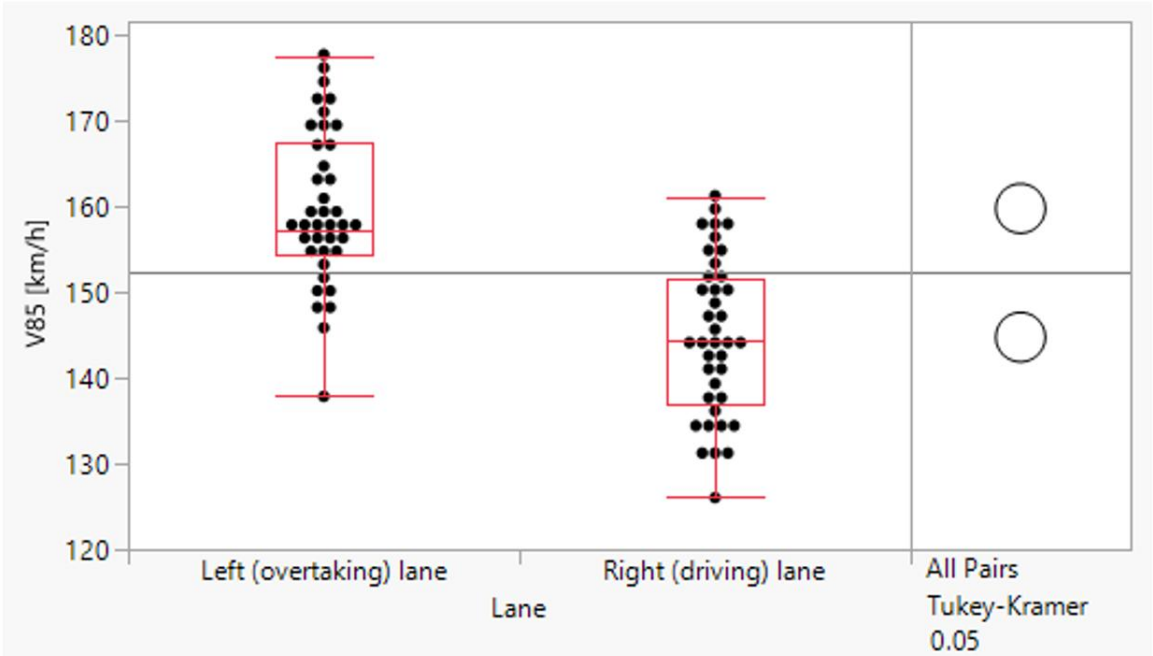

Level		Mean	Std Error
Left (overtaking) lane	A	159.71	1.4509
Right (driving) lane	B	144.72	1.4509

Level	- Level	Difference	Std Err Dif	Lower CL	Upper CL	p-Value
Left (overtaking) lane	Right (driving) lane	14.98886	2.051907	10.90213	19.07559	<.0001*

Figure 4 – Assessment of statistically significant differences in measured speeds between left and right motorway lanes using the Tukey–Kramer test

Analysis of the relationship between operating speed and identified variables for the right (driving) lane

To investigate the relationships between operating vehicle speed and continuous variables in the right (driving) lane, variables that satisfied the normality assumption were analysed using the Pearson correlation coefficient, whereas those that did not were assessed with Spearman's rank–order correlation. The results of both correlation analyses are presented in *Table 2*, showing the strength and direction of the associations between operating speed and each continuous variable.

Table 2 – Pearson and Spearman correlation results for continuous variables – right (driving) lane

Continuous variables	Test used	Pearson coefficient/Spearman's ρ	Significance level (*p*–value)
Total tunnel length in the last 20 km	Spearman	−0.1931	0.3445
Previous object distance	Spearman	0.0855	0.6779
Following object distance	Spearman	−0.1967	0.3355
Longitudinal slope	Pearson	−0.05464	0.7909
Heavy goods vehicles share (left lane)	Spearman	−0.1137	0.5803
Heavy goods vehicles share (right lane)	Pearson	0.021603	0.9166
AADT	Spearman	−0.2447	0.2283
ASDT	Pearson	−0.19889	0.3300
Traffic flow density (left lane)	Spearman	−0.4338	0.0268*
Traffic flow density (right lane)	Spearman	−0.4989	0.0095*

The correlation analysis confirmed that, in the right (driving) lane, operating speed (V85) is most strongly influenced by traffic flow density. Both traffic flow density (right lane) ($\rho = -0.4989$, $p = 0.0095$) and traffic flow density (left lane) ($\rho = -0.4338$, $p = 0.0268$) demonstrated statistically significant negative correlations with V85, indicating that higher vehicle concentrations in either lane reduce the operating speeds of passenger cars in the right lane. The findings corroborate earlier research [31], in which traffic density also emerged as the dominant factor (right lane: $\rho = -0.7043$, $p = 0.0005$; left lane: $\rho = -0.7901$, $p < 0.0001$). However, the strength of the correlation is somewhat reduced in the enlarged dataset, suggesting that while density remains the primary explanatory factor, adding additional cross–sections introduced greater variability in speed–density relationships.

Other continuous variables, including total tunnel length in the last 20 km, previous object distance, following object distance, longitudinal slope, heavy goods vehicle share (left and right lanes), AADT and ASDT, did not reach statistical significance ($p > 0.05$) in the present analysis. This again aligns with the first study, where most of these factors also showed weak or non–significant correlations with V85. The only exception was ASDT, which was significant in the earlier dataset ($\rho = -0.5525$, $p = 0.0115$) [31] but no longer retains significance in the expanded analysis ($\rho = -0.1989$, $p = 0.3300$). This reduction in explanatory power may be attributed to the broader sample of locations, which diluted the strong seasonal effects observed in the initial, smaller dataset.

Overall, the results reinforce the conclusion from the first research that operating speeds in the right lane are primarily shaped by traffic density, while other geometric and contextual variables exert a less pronounced influence. The expanded dataset demonstrates that density effects are solid across a wider range of locations, although the correlation strength is moderated compared to the initial findings.

Operating speeds were compared across the multiple levels of each categorical variable by applying analysis of variance (ANOVA). This technique made it possible to determine whether significant differences existed between the operating speeds associated with the different categories. The corresponding ANOVA results are presented in *Figure 5*.

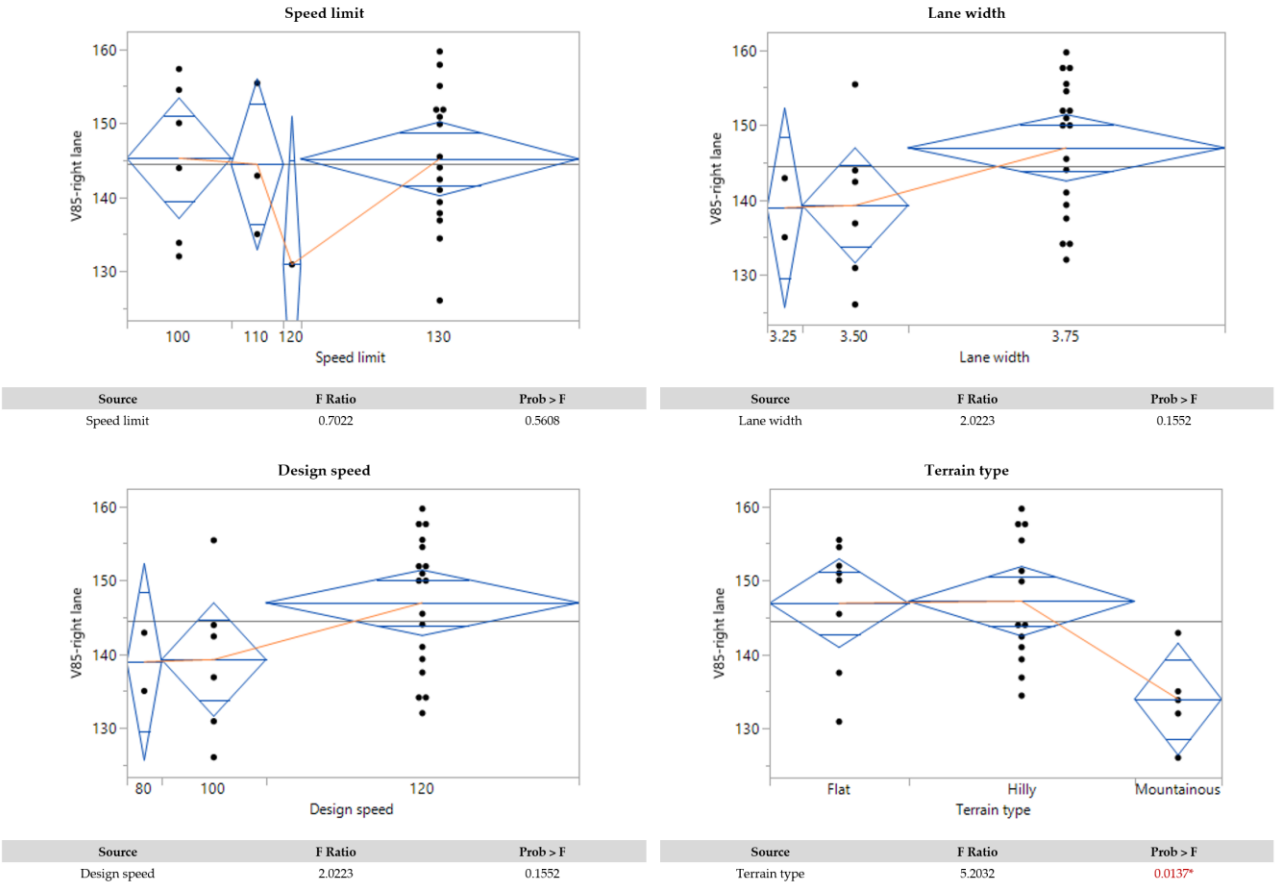

Figure 5 – Results of ANOVA for multi–level categorical variables – right (driving) lane

The ANOVA results for categorical variables in the right (driving) lane indicate a statistically significant difference in mean V85 across terrain types (F = 5.2032, p = 0.0137), i.e. the average 85th percentile speeds differ between flat, hilly and mountainous sections rather than implying a direct causal effect of "terrain" per se. By contrast, speed limit (F = 0.7022, p = 0.5608), lane width (F = 2.0223, p = 0.1552) and design speed (Vp) (F = 2.0223, p = 0.1552) do not show statistically significant differences in mean V85 (p > 0.05). Compared with the previous research [31], where none of these categorical variables reached significance and terrain type only showed a non–significant tendency (F = 2.4380, p = 0.1172), the enlarged sample has strengthened the evidence that means vary by terrain category. This change is plausibly attributable to the increased number and geographic spread of locations, which improves the power to detect between–group differences. It is important to emphasise that the ANOVA result signals between–category differences in mean V85; these differences likely reflect covarying location characteristics (alignment geometry, sight distance, longitudinal slopes, etc.) rather than a single mechanistic effect of the nominal terrain label. For completeness, pairwise post–hoc comparisons, the Tukey–Kramer test is conducted to identify which terrain pairs differ significantly and to quantify the magnitude of those differences (*Figure 6*).

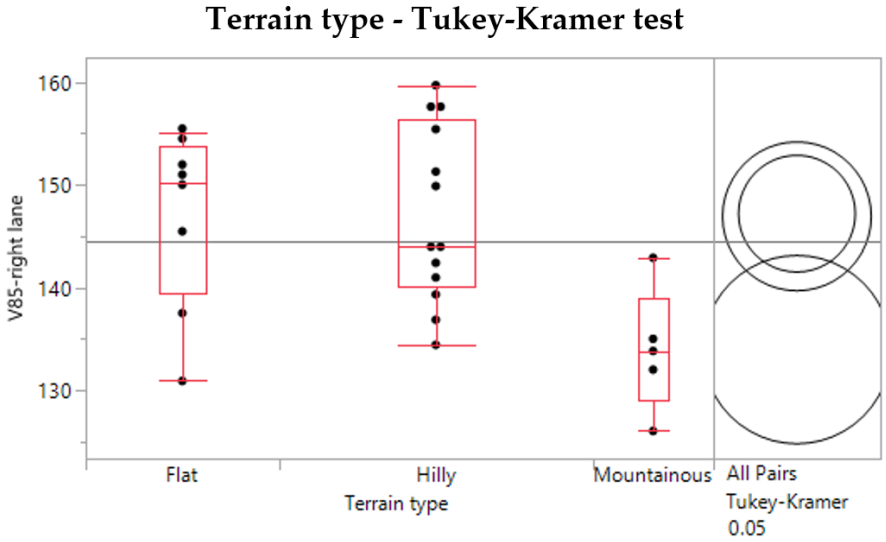

Level		Mean	Std Error
Hilly	A	147.17	2.2684
Flat	A	146.91	2.8916
Mountainous	B	133.95	3.6576

Level	- Level	Difference	p-Value
Hilly	Mountainous	13.22405	0.0143*
Flat	Mountainous	12.96611	0.0276*
Hilly	Flat	0.25794	0.9973

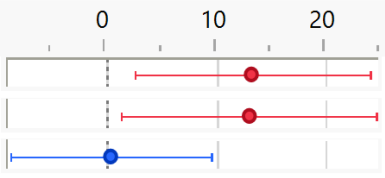

Figure 6 – Analysis of terrain type differences using the Tukey–Kramer test – right lane

The Tukey–Kramer test was applied to more thoroughly analyse the significant ANOVA result for terrain type in the right (driving) lane. The analysis revealed that mean operating speeds on mountainous terrain (133.95 km/h, SE = 3.66) were significantly lower compared with both hilly terrain (147.17 km/h, SE = 2.27; difference = 13.22 km/h, p = 0.0143) and flat terrain (146.91 km/h, SE = 2.89; difference = 12.97 km/h, p = 0.0276). No significant difference was observed between hilly and flat terrain (difference = 0.26 km/h, p = 0.9973). These results suggest that the main distinction lies between mountainous terrain and the other two categories, where operating speeds of passenger cars are considerably lower. This outcome is consistent with expectations, since mountainous areas typically feature steeper gradients, more frequent vertical and horizontal alignment constraints, and more demanding driving conditions, all contributing to reduced speeds in the right lane.

Analysis of the relationship between operating speed and identified variables for the left (overtaking) lane

Following the same approach used for the right (driving) lane, the relationships between operating vehicle speed and continuous variables in the left (overtaking) lane were examined. Variables that met the normality assumption were analysed using the Pearson correlation coefficient, while Spearman's rank–order correlation was applied to those that did not. *Table 3* presents the results of both correlation analyses, indicating the strength and direction of the associations between operating speed and each continuous variable.

Table 3 – Pearson and Spearman correlation results for continuous variables – left (overtaking) lane

Continuous variables	Test used	Pearson coefficient/Spearman's ρ	Significance level (*p*–value)
Total tunnel length in the last 20 km	Spearman	−0.1639	0.4235
Previous object distance	Spearman	0.0123	0.9524
Following object distance	Spearman	0.0219	0.9155
Longitudinal slope	Pearson	−0.021	0.9189
Heavy goods vehicles share (left lane)	Spearman	0.0204	0.9212
Heavy goods vehicles share (right lane)	Pearson	−0.02688	0.8963
AADT	Spearman	−0.0585	0.7764
ASDT	Pearson	−0.0486	0.8136
Traffic flow density (left lane)	Spearman	−0.3302	0.0994
Traffic flow density (right lane)	Spearman	−0.4124	0.0363*

For the left (overtaking) lane, the results indicate that traffic flow density remains the most relevant variable, although the strength of correlations is weaker compared to the earlier research [31]. Specifically, traffic flow density (right lane) showed a significant negative association with V85 ($\rho = -0.4124$, $p = 0.0363$), while traffic flow density (left lane) exhibited a weaker, non–significant correlation ($\rho = -0.3302$, $p = 0.0994$). These results suggest that passenger–car operating speeds in the overtaking lane are still sensitive to surrounding traffic concentration, but the explanatory power of density has decreased relative to the first research. In the earlier analysis [31], density effects were much stronger (left lane: $\rho = -0.7434$, $p = 0.0002$; right lane: $\rho = -0.6661$, $p = 0.0013$), indicating that the addition of new locations has introduced greater variability and thereby moderated the strength of observed relationships.

Other continuous variables did not show statistically significant correlations in the present dataset. Notably, heavy goods vehicles share (left lane), which previously showed a strong positive correlation with V85 ($\rho = 0.6152$, $p = 0.0039$) [31], no longer demonstrates significance ($\rho = 0.0204$, $p = 0.9212$). Similarly, ASDT, which was significant in the earlier research ($\rho = -0.4649$, $p = 0.0389$) [31], no longer exhibits explanatory power ($\rho = -0.0486$, $p = 0.8136$). These shifts suggest that lane–specific effects of heavy vehicles and seasonal demand, which were more pronounced in the smaller dataset, have been diluted by the broader coverage of locations in the expanded research. Geometric and contextual factors, such as total tunnel length in the last 20 km, previous object distance, following object distance and longitudinal slope, remained non–significant in both analyses.

Overall, the results confirm the functional distinction of the left lane: while operating speeds remain higher and more homogeneous than the right lane, they are still constrained by traffic flow density, particularly conditions in the adjacent right lane. The expanded dataset thus corroborates the earlier research findings but also shows that some previously significant variables (e.g. heavy vehicle share, ASDT) lose their explanatory value when a larger and more diverse set of locations is considered.

Operating speeds were compared across the multiple levels of each categorical variable by applying analysis of variance (ANOVA). This technique made it possible to determine whether significant differences existed between the operating speeds associated with the different categories. The corresponding ANOVA results are presented in *Figure 7*.

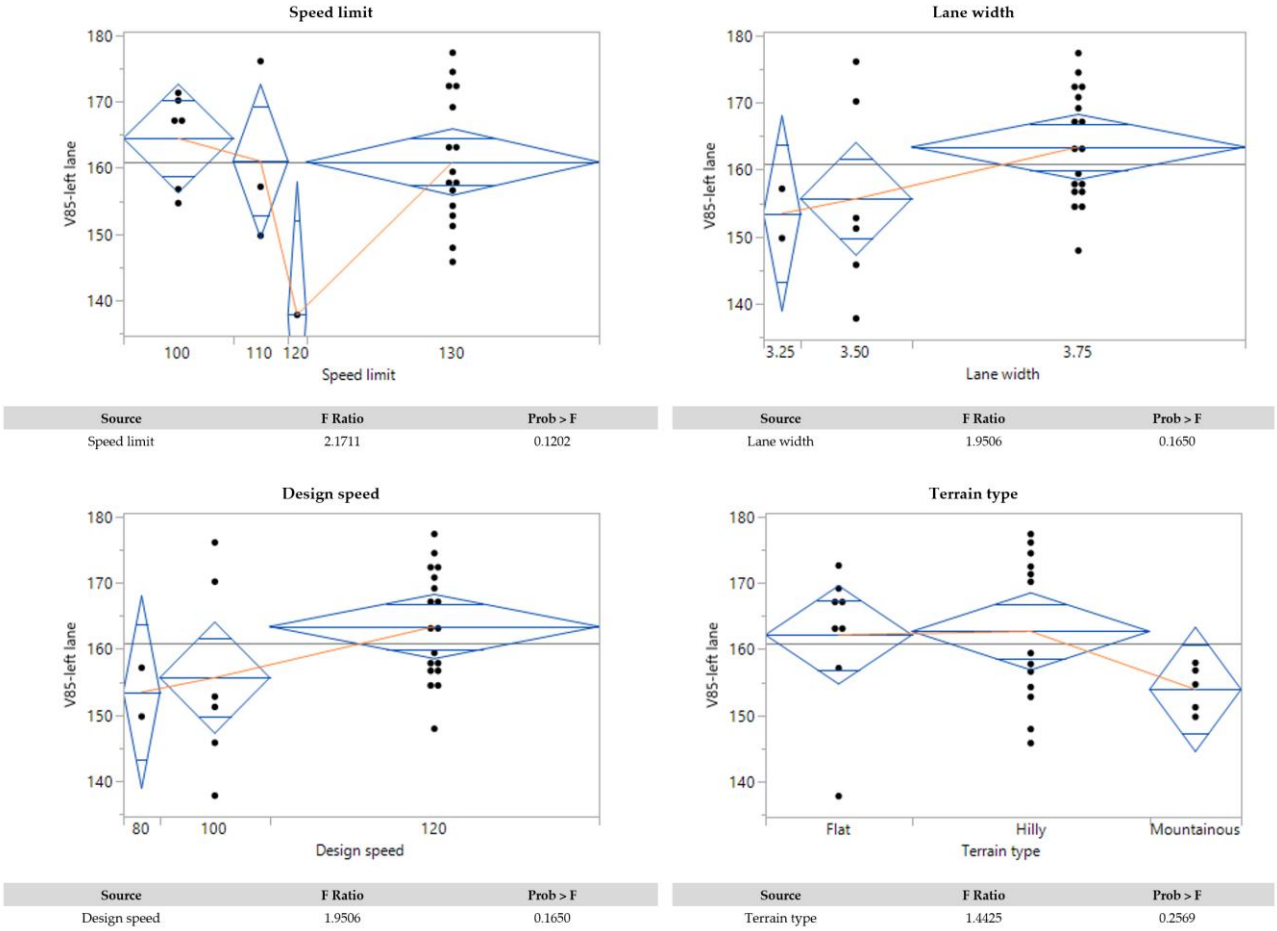

Source	F Ratio	Prob > F
Speed limit	2.1711	0.1202

Source	F Ratio	Prob > F
Lane width	1.9506	0.1650

Source	F Ratio	Prob > F
Design speed	1.9506	0.1650

Source	F Ratio	Prob > F
Terrain type	1.4425	0.2569

Figure 7 – Results of ANOVA for multi–level categorical variables – left (overtaking) lane

The ANOVA results for the left (overtaking) lane indicate that no tested categorical variables exhibited a statistically significant difference in mean V85 between their respective categories. Specifically, speed limit ($F = 2.1711$, $p = 0.1202$), lane width ($F = 1.9506$, $p = 0.1650$), design speed (Vp) ($F = 1.9506$, $p = 0.1650$) and terrain type ($F = 1.4425$, $p = 0.2569$) all yielded p–values greater than 0.05. These results suggest that, in the overtaking lane, passenger–car operating speeds remain relatively homogeneous across different design and environmental categories, reflecting the functional role of this lane as a facility for faster traffic flows where drivers' behaviour is less constrained by categorical roadway features.

Compared with the previous research [31], the present findings are broadly consistent. None of the categorical factors reached statistical significance in the smaller dataset, although terrain type showed a near–significant trend ($F = 2.6842$, $p = 0.0970$). This tendency is no longer evident in the expanded dataset, as the effect of terrain differences becomes weaker and statistically insignificant. The stability of non–significant results across both studies indicates that categorical design and environmental variables have limited explanatory power for variations in V85 in the left lane, where operating speeds are more strongly associated with continuous traffic–flow variables, as evidenced by the correlation analysis.

3.2 Operating speed prediction model development

To develop operating speed prediction models of passenger cars on dual–carriageway road tangents, all identified explanatory variables were considered regardless of whether their initial statistical examination showed significant associations. While some variables had previously been analysed in categorical form, namely speed limit, lane width, design speed and terrain type, they were incorporated into the modelling process either as continuous variables or transformed into dummy variables in the case of terrain type. Specifically, the terrain type variable was simplified into two binary categories, mountainous and flat, to capture the key contrasts identified in the ANOVA and post–hoc analyses. This approach ensured that all potentially relevant infrastructural, traffic and environmental variables were included in the regression

framework, allowing the modelling process to determine their ultimate explanatory contribution. Separate models were subsequently developed for the right (driving) and left (overtaking) lanes, reflecting the distinct operating speed dynamics confirmed in the earlier analyses.

Model development – Right (driving) lane

The development of the multiple linear regression model for the right (driving) lane was based on a systematic selection of candidate predictors. Variables were first evaluated through correlation analysis, ANOVA and Tukey–Kramer tests to determine their potential association with operating speed (V85). Variables that demonstrated statistical significance or were strongly supported by traffic flow theory and road design principles were selected for further analysis. Categorical variables like speed limit, lane width and design speed were represented as continuous variables, while terrain type was converted into a binary dummy variable contrasting mountainous sections with flat and hilly sites. Descriptive statistics of all candidate variables are provided in Appendix B.

The correlation matrix (Appendix C) was examined to identify potential multicollinearity. Several strong pairwise correlations were observed: lane width and design speed (Vp) were perfectly correlated (r=1.00), confirming redundancy; therefore, only one could be retained. Similarly, AADT and ASDT were highly correlated (r=0.85), and only ASDT was considered for modelling due to its seasonal sensitivity and slightly stronger correlation with V85. Finally, traffic flow density (left lane) and traffic flow density (right lane) were also strongly correlated (r=0.89), and only one was included to avoid overlapping explanatory effects. These steps ensured that the final set of predictors preserved statistical validity while maintaining conceptual diversity.

Variance inflation factors (VIF) were computed for all variables in the final model to evaluate potential collinearity. All VIF values remained comfortably below the conventional threshold of 5, with lane width having the highest value at 2.84. These results indicate that multicollinearity is not problematic and support the estimated coefficients' reliability.

The final regression model (*Table 4*) for the right lane included eight predictors: total tunnel length in the last 20 km, speed limit, lane width, following object distance, longitudinal slope, terrain type–mountainous, ASDT and traffic flow density (left lane). Several of these predictors were statistically significant at the 95% confidence level ($p < 0.05$), while speed limit ($p = 0.064$) and terrain type–mountainous ($p = 0.062$) were retained due to their conceptual relevance and contribution to explanatory balance.

The set of retained predictors is consistent with prior multilane and four–lane studies that emphasise lane–specific effects and the importance of both geometric and traffic variables. Earlier research on four–lane/divided highways found that lane discipline and interactions between adjacent lanes materially affect operating speeds, and therefore, lane-based modelling is appropriate. For example, research developed separate models for inside and outside lanes on four–lane rural highways and highlighted the need for lane–specific treatments in speed prediction [28]. Similarly, more recent studies on four–lane divided facilities report that geometric parameters (e.g. lane/tangent geometry) and traffic variables are central predictors in lane–based models and obtain comparable explanatory power (R^2 in the 0.7–0.9 range) when free–flow criteria are strictly applied [37]. Specific coefficient signs and magnitudes in the present right–lane model align with established findings. The strongly negative coefficient for traffic flow density (left lane) mirrors observations that higher concentrations in the adjacent overtaking lane reduce available overtaking opportunities and depress speeds in the driving lane; an inter–lane interaction highlighted in four–lane studies [37]. The positive association with lane width concurs with prior evidence that wider travelled way elements increase perceived driving comfort and are associated with higher operating speeds on dual–carriageway roads [29]. The observed importance of the longitudinal slope (positive coefficient in the present model) is also supported by several multilane studies that identify grade as a significant predictor of speed, particularly when slopes exceed small thresholds that drivers perceive as notable [38, 39]. Finally, including total tunnel length in the last 20 km and following object distance as meaningful predictors extends the literature by showing how the recent driving environment (e.g. prolonged tunnel exposure) and proximity to downstream features can influence right–lane operating speed on tangents. While such contextual variables have been considered in some highway speed–profile models, their joint significance underlines the value of combining infrastructural, traffic and environmental variables in lane–specific speed prediction for dual–carriageway roads.

The model achieved a coefficient of determination of $R^2 = 0.82$ and an $R^2_{Adj} = 0.74$, indicating that 74% of the variability in operating speed is explained after adjusting for model complexity. The root mean square error (RMSE) of 4.85 and the relatively low sum of squares for error (SSE = 400.42) further confirm the accuracy

of predictions. With 26 observations and nine estimated parameters, the degrees of freedom for error (DFE) were 17, providing sufficient residual variability for reliable inference. The Mallows' Cp statistic equalled 9, closely corresponding to the number of predictors, indicating a parsimonious yet effective model.

Overall, the right–lane model demonstrates that V85 on dual–carriageway road tangents is shaped by a combination of infrastructural, traffic and environmental factors. The positive coefficients for lane width, longitudinal slope and ASDT highlight the influence of roadway design and traffic volume on speed choice, while the negative effect of traffic flow density (left lane) illustrates how interactions with the overtaking lane constrain speeds in the driving lane. Including total tunnel length in the last 20 km and following object distance underscores the importance of contextual conditions in shaping drivers' behaviour in tangent sections.

Table 4 – Regression results – operating speed prediction model for right (driving) lane

Variable	Estimate	Std error	*p*–value	Lower 95%	Upper 95%	VIF
Intercept	−13.48	39.6908	1	−97.22	70.26	——
Total tunnel length in the last 20 km	0.007	0.0019	0.00220	0.00	0.01	2.22
Speed limit	–0.17	0.0865	0.06360	−0.35	0.01	1.37
Lane width	50.36	10.2602	0.00010	28.72	72.01	2.84
Following object distance	−0.0009	0.0004	0.03500	0.00	0.00	1.33
Longitudinal slope	1.93	0.6476	0.00850	0.56	3.29	1.38
Terrain type–mountainous	–6.85	3.4333	0.06230	−14.09	0.39	2.02
ASDT	0.0005	0.0002	0.02600	0.00	0.00	1.90
Traffic flow density (left lane)	–5.41	0.9584	0.00003	−7.43	−3.38	2.14

R^2	0.82
R^2_{Adj}	0.74
RMSE	4.85
Mean of response	144.55
SSE	400.42
DFE	17
Cp	9
Observations	26

Model development – Left (overtaking) lane

The model for the left (overtaking) lane was developed using the same structured procedure described previously for the right (driving) lane. Candidate predictors were examined for their association with operating speed (V85) through correlation analysis, ANOVA and Tukey–Kramer tests, and were retained based on statistical significance or theoretical justification. Categorical variables such as speed limit, lane width and design speed (Vp) were treated as continuous variables, while terrain type was recoded into dummy variables. Descriptive statistics of all variables are provided in Appendix B.

The correlation matrix (Appendix C) assessed pairwise relationships among predictors. As with the right–lane model, strong correlations were identified between AADT and ASDT (r = 0.85), and between lane width and design speed (Vp) (r = 1.00), leading to the exclusion of redundant variables to avoid multicollinearity.

Variance inflation factors (VIF) confirmed the stability of the selected predictors, with all values well below the threshold of 5 (highest VIF = 2.18 for lane width).

The final model (*Table 5*) retained six predictors: total tunnel length in the last 20 km, speed limit, lane width, longitudinal slope, ASDT and traffic flow density (left lane). Several variables were statistically significant at the 95% confidence level ($p < 0.05$). Positive coefficients were obtained for lane width, longitudinal slope, ASDT and total tunnel length, reflecting their contribution to higher operating speeds, whereas speed limit and traffic flow density (left lane) were associated with lower V85 values.

The model achieved a coefficient of determination of $R^2 = 0.71$ and an $R^2_{Adj} = 0.62$, with an RMSE of 6.36. While this explanatory power is acceptable, it is notably lower than that of the right–lane model. The relatively modest fit can be attributed to greater variability in overtaking–lane speeds, and contextual factors related to driver behaviour and speed enforcement practices. In Croatia, legal provisions on speed enforcement stipulate a tolerance of 10% for measured speeds above 100 km/h, meaning that at the motorway limit of 130 km/h, enforcement only applies at 143 km/h and above [44]. In practice, drivers are rarely penalised below approximately 160 km/h as indicated on vehicle speedometers. This regulatory tolerance reduces the deterrent effect of posted speed limits, particularly in the overtaking lane, where drivers commonly travel at higher speeds. Consequently, the statistical association between geometric or traffic–flow variables and actual operating speed is attenuated, which partly explains the reduced explanatory power of the overtaking–lane model.

These results are consistent with international findings that overtaking lane speeds are more difficult to predict with high precision. Studies on multilane facilities have shown that inside/overtaking lanes often exhibit greater variability due to discretionary driver behaviour and enforcement regimes [40, 41]. The strong effect of traffic flow density (left lane) aligns with prior evidence that lane–specific congestion influences overtaking–lane speeds disproportionately [42]. Nevertheless, including traffic and geometric variables provides a balanced representation of overtaking–lane dynamics, even though some speed variance remains unexplained due to enforcement–related behavioural factors unique to the Croatian context [43].

Table 5 – Regression results – operating speed prediction model for left (overtaking) lane

Variable	Estimate	Std error	*p*–value	Lower 95%	Upper 95%	VIF
Intercept	−63.1435	43.7565	1	–154.7269	28.4400	——
Total tunnel length in the last 20 km	0.0094	0.0025	0.0012	0.0042	0.0146	2.14
Speed limit	−0.2211	0.1036	0.0462	–0.4380	–0.0041	1.14
Lane width	68.2409	11.7737	<0.0001	43.5982	92.8835	2.18
Longitudinal slope	1.9644	0.8111	0.0256	0.2668	3.6621	1.26
ASDT	0.0006	0.0002	0.0186	0.0001	0.0011	1.73
Traffic flow density (left lane)	−6.4552	1.2003	<0.0001	–8.9674	–3.9429	1.95

R^2	0.71
R^2_{Adj}	0.62
RMSE	6.36
Mean of response	60.84
SSE	768.28
DFE	19
Cp	7
Observations	26

3.3 Operating speed prediction model validation

Residual analysis was performed to evaluate the validity of the developed operating speed prediction models and confirm compliance with multiple linear regression assumptions. Residual scatter plots, histograms and frequency distributions (*Figures 8* and *9*) demonstrated that residuals were evenly distributed around the zero line and symmetrically. The Shapiro–Wilk tests (*Tables 6* and *7*) confirmed normality for both models, with non–significant results obtained for the right lane (W = 0.98, p = 0.85) and the left lane (W = 0.97, p = 0.75), indicating no departure from the assumption of normally distributed residuals. Together, the graphical and statistical evidence support the adequacy of the models with respect to residual behaviour.

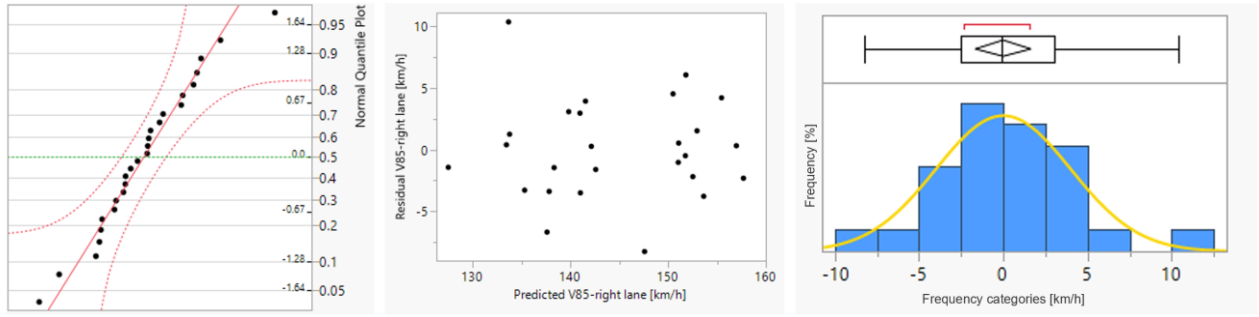

(a) *(b)* *(c)*

Figure 8 – Right (driving) lane: (a) scatter plots for assessing the performance of the developed model, (b) distribution of residuals, (c) frequency distribution of residuals

Table 6 – Residual distribution analysis via the Shapiro–Wilk test – right (driving) lane

	W	***p*–value**
Shapiro–Wilk	0.98	0.85

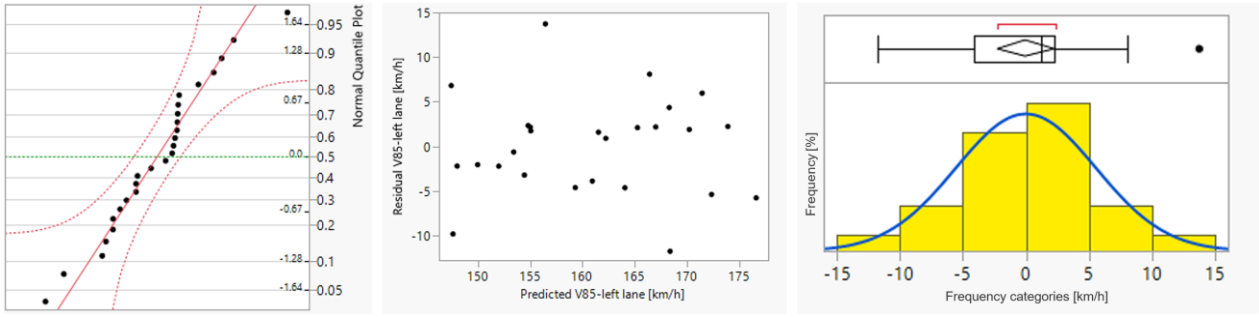

(a) *(b)* *(c)*

Figure 9 – Left (overtaking) lane: (a) scatter plots for assessing the performance of the developed model, (b) distribution of residuals, (c) frequency distribution of residuals

Table 7 – Residual distribution analysis via the Shapiro–Wilk test – left (overtaking) lane

	W	***p*–value**
Shapiro–Wilk	0.97	0.75

An external validation process was conducted using 13 tangent locations not included in the model development phase to assess predictive performance and generalisability further. For each location, the measured operating speed (V85–test) was compared with the model–predicted operating speed (V85–predicted), as presented in *Table 8.* In addition to the direct comparison, the absolute difference [km/h] and relative deviation [%] were computed for both the right (driving) and left (overtaking) lanes to provide a more comprehensive evaluation of model accuracy.

Table 8 – Model validation results

Location	Direction	V85−Right lane−test [km/h]	V85− Right lane−predicted [km/h]	Absolute difference−right lane [km/h]	Absolute deviation−right lane [%]	V85−Left lane−test [km/h]	V85−Left lane−predicted [km/h]	Absolute difference−left lane [km/h]	Absolute deviation−left lane [%]
L2	Blato na Cetini − Bisko	142	153.17	11.06	7.79%	158	167.67	9.56	6.05%
L5	Donja Zdenčina − Jastrebarsko	131	148.70	17.92	13.70%	148	160.56	12.13	8.17%
L8	Gospić − Gornja Ploča	134	147.83	13.42	9.98%	157	162.83	6.01	3.83%
L15	Križ−Popovača	148	149.74	1.59	1.07%	156	166.63	10.85	6.97%
L18	Nova Gradiška − Lužani	141	134.34	6.74	4.78%	161	156.41	4.21	2.62%
L21	Zagreb − Karlovac	144	149.76	5.48	3.79%	159	163.12	3.68	2.31%
L23	Zagreb − Karlovac	147	146.61	0.53	0.36%	154	160.39	6.24	4.05%
L27	Slavonski Brod − Babina Greda	144	151.71	7.45	5.16%	155	165.83	10.48	6.75%
L28	Babina Greda − Slavonski Brod	161	149.23	11.67	7.25%	169	164.54	4.41	2.61%
L29	Zagreb − Slavonski Brod	147	134.14	12.66	8.62%	156	146.34	9.63	6.17%
L32	Josipdol − Bosiljevo	136	134.67	1.47	1.08%	150	151.81	1.35	0.90%
L35	Šibenik − Split	157	157.55	0.88	0.56%	165	173.74	9.24	5.61%
L38	Posedarje − Šibenik	153	148.63	4.55	2.97%	158	167.27	9.10	5.75%
			Average absolute deviation:		**5.16%**				**4.75%**

The validation results show that the developed models achieved satisfactory prediction accuracy. For the right–lane model, the average absolute deviation across all validation sites was 5.16%, while the corresponding average deviation was slightly lower at 4.75% for the left-lane model. These values indicate that, on average, the predicted operating speeds deviated from observed speeds by approximately 5%. The largest deviations occurred at certain sites (e.g. Donja Zdenčina – Jastrebarsko and Zagreb – Slavonski Brod), where deviations exceeded 10%, while the most accurate predictions showed below 1%. Importantly, the deviations were balanced, with no evidence of systematic overestimation or underestimation, suggesting that both models exhibit solid predictive behaviour across diverse locations.

Compared with the single–carriageway model developed in earlier research [33], the dual–carriageway models show somewhat higher average deviations, which can be explained by behavioural differences between driving and overtaking lanes. For the right lane, prediction accuracy is largely determined by traffic flow characteristics, which the selected predictors adequately capture. By contrast, the left–lane model exhibits greater variability due to discretionary driver behaviour and the effects of enforcement tolerance in Croatia. As current legislation [44] allows a 10% tolerance above 100 km/h, speeds up to approximately 143 km/h at a posted limit of 130 km/h are not subject to penalties. In practice, drivers are rarely sanctioned for speeds below ~160 km/h (as indicated on vehicle speedometers), which reduces the deterrent effect of posted speed limits and leads to higher and more variable speeds in the overtaking lane. This enforcement context partly explains why the left–lane model achieves only moderate explanatory power ($R^2_{Adj} = 0.62$) and exhibits larger local deviations.

Nevertheless, the validation outcomes demonstrate that both models generalise reasonably well beyond the development dataset. Including infrastructural, traffic and environmental variables provides a balanced explanatory framework that accounts for the majority of variability in operating speeds. The observed deviations, while somewhat higher than in single–carriageway contexts, remain within acceptable bounds for practical applications. The models are therefore suitable for road design evaluation, speed management and safety analysis on dual–carriageway tangents, while acknowledging the influence of driver behaviour and enforcement policy on overtaking lane speed prediction.

4. CONCLUSION

This research developed lane–specific multiple linear regression models for predicting passenger car operating speeds (V85) on dual–carriageway road tangents. Models were estimated separately for the right (driving) and left (overtaking) lanes using a dataset expanded from previous research [31] collected with drone video surveys and post–processed under strict criteria. Predictor candidates covered infrastructural, traffic and environmental factors (14 variables), and model development followed a stepwise se*lection procedure with multicollinearity diagnostics and out–of–sample validation*. Model performance and residual diagnostics were examined to assess explanatory capability and practical applicability.

Key quantitative outcomes are as follows. The final model for the right (driving) lane explains 82% of the variance in site–level V85 ($R^2 = 0.82$) with RMSE = 4.85; the left (overtaking) lane model explains 71% of the variance ($R^2 = 0.71$) with RMSE = 6.36. Residual distributions for both models do not depart from normality (Shapiro–Wilk: right $W = 0.98$, $p = 0.85$; left $W = 0.97$, $p = 0.75$). External validation on the reserved test set indicates average absolute deviations of ≈5.16% (right lane) and ≈4.75% (left lane) between predicted and observed V85 values, with both over– and under–predictions present and no clear systematic bias across sites.

Despite these acceptable aggregate statistics, the analysis revealed only a limited number of explanatory variables with stable, statistically significant associations with V85. Traffic flow density (lane–specific) emerged as the most consistent predictor in both lanes. A smaller set of geometric/contextual variables (lane width, longitudinal slope, ASDT and recent tunnel exposure) entered the final specifications but contributed more modestly. Many candidate variables, including several categorical design indicators and posted speed limit, showed weak or inconsistent relationships with V85. Consequently, while the models capture a substantial share of variance, a non–negligible portion of speed variability remains unexplained at the location level.

However, several contextual and behavioural factors plausibly limit how geometric and traffic descriptors alone can explain V85, particularly in the overtaking lane. First, the enforcement environment on Croatian motorways reduces the effective deterrence of posted limits: speed control relies heavily on mobile operations and unmarked “interceptor” patrols whose presence is spatially and temporally unpredictable. In addition, Croatian legislation [44] applies a measurement tolerance above 100 km/h (10% allowance), which raises the threshold drivers can expect sanctioning and weakens the link between posted limits and realised free–flow speeds. Empirical syntheses show that more visible and sustained enforcement (fixed cameras and section average control) substantially reduces mean and 85th percentile speeds and speed variability, whereas mobile or intermittent enforcement produces smaller, more localised effects [45, 46]. Second, vehicle automation and assistance systems alter speed choices that reduce sensitivity to local geometric cues. Cruise control and, increasingly, adaptive cruise control (ACC) allow drivers to maintain a chosen set–speed for long periods; field studies find that speeding beyond the posted limits is more common among drivers limits when ACC (and lane–centring variants) is engaged, and that these systems reduce short–term speed variability while shifting the distribution of speeds upward in some contexts [47, 48]. Third, fleet and driver–type effects introduce behavioural heterogeneity not captured by standard geometric or aggregate traffic variables. Evidence from work–related driving research indicates that company–car drivers tend to accept higher speeds and more frequent speeding than private–car drivers, plausibly because personal fuel–cost disincentives are weaker; survey and observational studies report substantially higher self–reported and measured speeding among company–car cohorts [49, 50]. Newer, higher–performance vehicles (common in corporate fleets) also enable higher attainable and comfortable cruising speeds with less perceptible effort, further weakening correlations between V85 and infrastructure characteristics. These enforcement, technological and fleet/behavioural mechanisms make overtaking lane speeds less tightly linked to the local geometric and flow variables typically measured in field campaigns. They therefore help explain why relatively few candidate predictors showed stable statistical significance in the present models and why a non–negligible component of location–level variance remains unexplained.

The study also highlights several limitations that should guide future research. First, its geographic specificity must be acknowledged; the research was conducted on Croatian motorways and therefore reflects national infrastructure standards, enforcement practices and driver behaviour. Applying these results to different countries requires caution and prior calibration of local traffic characteristics, particularly because the share of foreign drivers was not identified. Second, the dataset was limited to favourable weather and daylight conditions, excluding nighttime driving, adverse weather or transitional light settings, which are known to affect speed choice and could reveal additional behavioural dynamics.

Furthermore, no direct measures of enforcement activity, technological adoption (e.g. cruise control, adaptive cruise control) or vehicle ownership typology (company vs. private cars) were included, even though these factors plausibly influenced the weak correlation between certain infrastructural variables and V85. Future studies would benefit from incorporating more precise and disaggregated measures, such as telematics–based indicators of automation use or records of local enforcement deployment.

Methodologically, stepwise multiple linear regression was adopted for its transparency and interpretability, but it remains limited in its ability to capture nonlinear effects or higher–order interactions among variables. Other approaches, such as generalised additive models, quantile regression or ensemble machine–learning methods, could be employed in future research, especially if paired with larger and more continuous datasets. Connected vehicle data, floating car data and other big–data sources hold promise for expanding sample size and temporal coverage, enabling exploration of dynamic speed patterns and more granular modelling of lane–specific behaviour.

Another important direction involves broadening the scope of application. While this research focused on tangent segments of dual–carriageway roads, transferability of the methodology to tangent–curve sequences, interchange approaches or transition zones (e.g. tunnel exits) could help determine how different geometric and contextual features interact with lane–specific speed choice. Moreover, explicit integration of human factors offers potential to improve predictive capability; operationalising variables such as overtaking frequency, perceived enforcement presence or driver workload through field observation or video analytics would provide a richer behavioural foundation. Embedding these enhanced models into decision–support tools would strengthen their utility for road designers, operators and policymakers, bridging the gap between predictive research and practical motorway safety management.

In conclusion, this study presents a methodologically rigid and empirically grounded contribution to developing lane–specific operating speed prediction models for passenger cars on dual–carriageway road tangents in Croatia. By separately modelling the right (driving) and left (overtaking) lanes, the research advances understanding of lane–differentiated speed behaviour on motorways and fills a notable gap in the existing body of literature. Although the explanatory strength of the models is influenced by enforcement practices, behavioural factors and technological trends in modern vehicles, the results offer meaningful insights into how infrastructural, environmental and traffic variables shape actual driving speeds under free–flow conditions. The findings provide a valuable reference for road design evaluation, traffic management and speed policy considerations, while establishing a solid basis for further refinement of predictive approaches. The operating speed models developed in this study, grounded in UAV-derived trajectory data and detailed predictors, offer a valuable input for modern Intelligent Transportation Systems (ITS) and adaptive speed management policy frameworks. For instance, real-time or near-real-time speed predictions could be integrated into motorway traffic management centres to trigger variable speed limit (VSL) advisories or regulatory changes when predicted operating speeds diverge from safe design thresholds. By dynamically aligning posted speed limits with empirical operating-speed behaviour under given geometry and traffic flow conditions, such systems may improve traffic flow homogenisation, reduce speed variability and enhance road safety [51, 52]. Furthermore, in a planning context, the models can support digital-twin simulations and pre-deployment assessments of VSL control zones, thereby enabling proactive policy design rather than purely reactive speed interventions. Ultimately, the adoption of data-driven speed management strategies based on empirical operating speed prediction can help motorway operators achieve a more consistent design-operating speed regime, strengthen the link between infrastructure design and enforcement, as well as contribute to safer, more efficient motorway performance. Future research should expand this work by incorporating larger and more diverse datasets, exploring behavioural and enforcement–related variables, and validating the models in broader international contexts, thereby enhancing their applicability and strengthening their role as practical tools for road safety and planning.

REFERENCES

[1] World Health Organization. *Global status report on road safety 2023*. Geneva, Switzerland: World Health Organization; 2023.

[2] SWOV Institute for Road Safety Research. *Speed and speed management*. The Hague, The Netherlands: SWOV; 2021.

[3] International Transport Forum. *Road safety annual report 2018*, OECD Publishing; 2018.

[4] Transport for NSW. Annual Report 2010. Sydney, Australia: Transport for NSW; 2011.

[5] European Automobile Manufacturers Association. *Road safety: Safe vehicles, safe drivers, safe roads*. Brussels, Belgium: ACEA; 2019.

[6] Ministry of the Interior, Republic of Croatia. Statistical overview of basic safety indicators and work results in 2022. Zagreb, Croatia: Ministry of the Interior; 2023.

[7] European Transport Safety Council. Reducing speeding in Europe, PIN Flash Report 36. Brussels, Belgium: ETSC; 2019.

[8] Karpenko M, Prentkovskis O, Skačkauskas P. Numerical simulation of vehicle tyre under various load conditions and its effect on road traffic safety. *Promet - Traffic&Transportation*. 2024;36(1):1–11. DOI: 10.7307/ptt.v36i1.265.

[9] Kabashkin I, Yatskiv I, Prentkovskis O, editors. Reliability and statistics in transportation and communication: human sustainability and resilience in the digital age. Lecture Notes in Networks and Systems, vol. 1337. Cham: *Springer*; 2025. DOI: 10.1007/978-3-031-87532-8.

[10] Lamm R, Psarianos B, Mailaender T. Highway design and traffic safety engineering handbook. New York, NY, USA: McGraw–Hill; 1999.

[11] Fitzpatrick K, Carlson P, Brewer MA. Exploration of the relationship between operating speed and roadway features on tangent sections. *J Transp Eng*. 2005;131(4):261–269.

[12] Elvik R. The power model of the relationship between speed and road safety: Update and new analyses. Oslo, Norway: Institute of Transport Economics; 2009.

[13] Ma X, et al. Long short–term memory neural network for traffic speed prediction. *Transp Res Part C*. 2015;54:187–197. DOI: 10.1016/j.trc.2015.03.014.

[14] Ma X, et al. Learning traffic as images: A deep convolutional neural network for large–scale transportation network speed prediction. *Sensors*. 2017;17(4):818. DOI: 10.3390/s17040818.

[15] Li YF, Chen MN, Lu XD, Zhao WZ. Research on optimised GA–SVM vehicle speed prediction model based on driver–vehicle–road–traffic system. *Sci China Technol Sci*. 2018;61:782–790. DOI: 10.1007/s11431-017-9213-0.

[16] Wang J, Chen R, He Z. Traffic speed prediction for urban transportation network: A path–based deep learning approach. *Transp Res Part C Emerg Technol*. 2019;100:372–385. DOI: 10.1016/j.trc.2019.02.002.

[17] Khajeh Hosseini M, Talebpour A. Traffic prediction using time–space diagram: A convolutional neural network approach. *Transp Res Rec*. 2019;2673(7):425–435. DOI: 10.1177/0361198119841291.

[18] Hashim IH, Abdel–Wahed TA, Moustafa Y. Toward an operating speed profile model for rural two–lane roads in Egypt. *J Traffic Transp Eng*. 2016;3(1):82–88. DOI: 10.1016/j.jtte.2015.09.005.

[19] Zuriaga AMP, García AG, Torregrosa FJC, D'Attoma P. Modeling operating speed and deceleration on two–lane rural roads with global positioning system data. *Transp Res Rec*. 2010;2171(1):11–20. DOI: 10.3141/2171-02.

[20] Choudhari T, Maji A. Effect of horizontal curve geometry on the maximum speed reduction: A driving simulator–based study. *Transp Dev Econ*. 2019;5:8. DOI: 10.1007/s40890-019-0082-8.

[21] Wang B, Hallmark S, Savolainen P, Dong J. Examining vehicle operating speeds on rural two–lane curves using naturalistic driving data. *Accid Anal Prev*. 2018;118:236–243. DOI: 10.1016/j.aap.2018.03.017

[22] Abdul–Mawjoud AA, Sofia GG. Development of models for predicting speed on horizontal curves for two–lane rural highways. *Arab J Sci Eng*. 2008;33(2):365–377.

[23] Memon RA, Khaskheli GB, Qureshi AS. Operating speed models for two–lane rural roads in Pakistan. C*an J Civ Eng*. 2008;35:443–453. DOI: 10.1139/L07-126.

[24] Shallam RDK, Ahmed MA. Operating speed models on horizontal curves for two–lane highways. Tra*nsp Res Procedia*. 2016;17:445–451. DOI: HTTPS://DOI.ORG/10.1016/j.trpro.2016.11.086.

[25] Malaghan V, Pawar DS, Dia H. Modeling operating speed using continuous speed profiles on two–lane rural highways in India. *J Transp Eng Part A Syst*. 2020;146:04020090. DOI: 10.1061/jtepbs.0000447.

[26] Sil G, Maji A, Nama S, Maurya AK. Operating speed prediction model as a tool for consistency–based geometric design of four–lane divided highways. *Transport*. 2019;34:796–807. DOI: 10.3846/transport.2019.10715.

[27] Alkherret AJ, AbuAddous MY, Al–Btoosh JA, Bani Baker MI. Modeling operating speed on multilane highways using GPS data. *Int Rev Civ Eng*. 2021;12(4):101–107. DOI: 10.15866/irece.v12i4.19743

[28] Gong H, Stamatiadis N. Operating speed prediction models for horizontal curves on rural four–lane highways. *Transp Res Rec*. 2008;2075:1–7. DOI: 10.3141/2075-01

[29] Maji A, Sil G, Tyagi A. 85th and 98th percentile speed prediction models of car, light, and heavy commercial vehicles for four–lane divided rural highways. *J Transp Eng Part A Syst*. 2018;144:05018001. DOI: 10.1061/JTEPBS.0000136

[30] Sil G, Nama S, Maji A, Maurya AK. Effect of horizontal curve geometry on vehicle speed distribution: A four–lane divided highway study. *Transp Lett*. 2019;12:713–722. DOI: 10.1080/19427867.2019.1695562.

[31] Vertlberg JL, Jakovljević M, Abramović B, Ševrović M. Determining factors influencing operating speeds on road tangents. *Appl Sci*. 2025;15:7549. DOI: 10.3390/app15137549.

[32] Krajewski R, Bock J, Kloeker L, Eckstein L. The HighD dataset: A drone dataset of naturalistic vehicle trajectories on German highways for validation of highly automated driving systems. *IEEE Conference on Intelligent Transportation Systems (ITSC)*, Maui, HI, USA, 2018, pp. 2118–2125. DOI: 10.1109/ITSC.2018.8569552

[33] Vertlberg JL, Jakovljević M, Abramović B, Ševrović M. Predicting operating speeds of passenger cars on single–carriageway road tangents. *Infrastructures*. 2025;10:221. DOI: 10.3390/infrastructures10080221.

[34] Ministry of the Sea, Transport and Infrastructure. *Ordinance on basic conditions that public roads outside settlements and their elements must meet from the point of view of traffic safety* (OG 110/2001 and 90/2022). Zagreb, Croatia: Ministry of the Sea, Transport and Infrastructure; 2022.

[35] Balakrishnan S, Sivanandan R. Influence of lane and vehicle subclass on free-flow speeds for urban roads in heterogeneous traffic. *Transp Res Procedia.* 2015;10:166–175. DOI: 10.1016/j.trpro.2015.09.066.

[36] Roh CG, Jeon H, Son B. Do heavy vehicles always have a negative effect on traffic flow? *Appl. Sci*. 2021; 11, 5520. DOI: 10.3390/app11125520.

[37] Sil G, Nama S, Maji A, Maurya AK. The 85th percentile speed prediction model for four–lane divided highways in ideal free flow condition. 2018. Conference of 97th Annual meeting of the Transportation Research Board, Washington, D.C. January, 2018 at: Washington, D.C.

[38] Eboli L, Guido G, Mazzulla G, Pungillo G. Experimental relationships between operating speeds of successive road design elements in two–lane rural highways. *Transport*. 2015;32(2):138–145. DOI: HTTPS://DOI.ORG/10.3846/16484142.2015.1110831.

[39] Lobo A, Amorim M, Rodrigues C, Couto A. Modelling the operating speed in segments of two–lane highways from probe vehicle data: A stochastic frontier approach. *J Adv Transp*. 2018;2018. DOI: 10.1155/2018/3540785.

[40] Himes S, Donnell E. Speed prediction models for multilane highways: simultaneous equations approach. *J Transp Eng.* 2010; 136:855–862. DOI: 10.1061/(ASCE)TE.1943-5436.0000149.

[41] Said D, Reyad F, Talaat H. Developing operating speed models for elevated multilane urban arterials using artificial neural networks. *J Eng Appl Sci*. 2023;70:123. DOI: 10.1186/s44147-023-00288-4.

[42] Ferko M, Pirdavani A, Babić D, Babić D. Exploring factors influencing speeding on rural roads: a multivariable approach. *Infrastructures*. 2024;9:222. DOI: 10.3390/infrastructures9120222.

[43] Zovak G, Kos G, Huzjan B. The driver behaviour and impact of speed on road safety on the motorways in Croatia. *Promet - Traffic&Transportation*. 2017;29(2):155–164. DOI: 10.7307/ptt.v29i2.2071.

[44] Croatian Bureau of Metrology. *Ordinance on metrological and technical requirements for speedometers in road traffic* (Official Gazette 60/2020). Zagreb, Croatia: Croatian Bureau of Metrology; 2020.

[45] Soole DW, Watson BC, Fleiter JJ. Effects of average speed enforcement on speed compliance and crashes: a review of the literature. *Accid Anal Prev*. 2013;54:46–56. DOI: 10.1016/j.aap.2013.01.018.

[46] Høye A. Speed cameras, section control, and kangaroo jumps – a meta–analysis. *Accid Anal Prev*. 2014;73:200–208. DOI: 10.1016/j.aap.2014.09.001.

[47] Monfort SS, et al. Speeding behaviour while using adaptive cruise control and lane centring in free flow traffic. *Traffic Inj Prev*. 2022;23:85–90. DOI: 10.1080/15389588.2021.2013476.

[48] Federal Highway Administration (FHWA). The effects of vehicle automation on driver engagement: the case of adaptive cruise control and mind wandering. *TechBrief* FHWA–HRT–21–017; 2021. DOI: 10.1177/0018720820974856.

[49] TRL. Work–related speeding: driving a necessary behavioural change. *TRL* blog/news. 2023. https://www.trl.co.uk/news/road–safety–week–work–related–speeding [Accessed 28th Sep. 2025].

[50] RAC Business. Rise in company car drivers speeding on motorways. Press release; 2016. https://media.rac.co.uk/rise–in–company–car–drivers–speeding–on–motorways–1592554 [Accessed 28th Sep. 2025].

[51] Papageorgiou, M, Kosmatopoulos, E, Papamichail, I. Effects of variable speed limits on motorway traffic flow. *Transportation Research Record: Journal of the Transportation Research Board*. 2008;2047(1):37-48. DOI: 10.3141/2047-05.

[52] Miloš J, et al. Influence of spatial placement of variable speed limit zones on urban motorway traffic control. *Promet - Traffic&Transportation.* 2022;34(4):511-522. DOI: 10.7307/ptt.v34i4.4073.

APPENDIX A – DUAL–CARRIAGEWAY LOCATIONS GENERAL DATA

Training set (26 locations)

Location	Motorway	Direction	Speed limit [km/h]	AADT [veh/day]	ASDT [veh/day]	Total sample size (all vehicle categories)		Filtered sample size (passenger cars)	
						Right lane [veh]	Left lane [veh]	Right lane [veh]	Left lane [veh]
L1	A1	Bisko − Blato na Cetini	130	5,253	11,059	739	391	113	86
L3	A1	Bosiljevo 2 − Ogulin	100	10,511	24,747	600	414	106	94
L4	A1	Ogulin − Bosiljevo 2	100	10,511	24,747	703	506	105	102
L6	A1	Jastrebarsko − Donja Zdenčina	130	20,603	34,474	585	863	79	86
L7	A1	Gornja Ploča − Gospić	100	9,255	22,581	468	243	73	25
L9	A1	Zadar Center − Zadar East	130	7,857	19,279	753	574	110	94
L10	A1	Zadar East − Zadar Center	130	7,857	19,279	770	611	106	85
L11	A2	Zabok − Zaprešić	130	9,999	15,473	355	137	86	29
L12	A2	Zaprešić − Zabok	130	9,999	15,473	502	232	108	43
L13	A3	Babina Greda − Županja	100	5,988	9,184	261	167	81	60
L14	A3	Županja − Babina Greda	100	5,988	9,184	211	87	32	62
L16	A3	Popovača − Križ	130	13,425	18,067	420	273	81	73
L17	A3	Lužani − Nova Gradiška	130	9,007	12,947	362	265	70	65
L19	A6	Delnice − Ravna Gora	110	7,981	13,233	438	158	99	54
L20	A6	Ravna Gora − Delnice	110	7,981	13,233	463	380	82	63
L22	A1	Karlovac − Zagreb	130	22,568	35,635	154	167	48	68
L24	A6	Karlovac − Rijeka	110	8,723	14,316	109	36	48	29
L25	A7	Rijeka − Rupa	130	4,458	8,960	63	4	40	4
L26	A4	Zagreb − Varaždin	100	7,322	12,119	89	31	33	22
L30	A3	Slavonski Brod − Zagreb	120	10,471	14,445	102	59	43	40
L31	A1	Bosiljevo − Josipdol	130	10,864	25,072	108	33	52	27
L33	A1	Gospić − Otočac	130	10,403	23,947	101	26	44	20
L34	A1	Gospić − Otočac	130	10,329	23,859	102	38	58	31
L36	A1	Zadar − Šibenik	130	7,928	17,180	95	45	54	30
L37	A1	Šibenik − Zadar	130	7,928	17,180	117	48	62	35
L39	A1	Šibenik − Posedarje	130	9,122	20,364	106	33	55	28
Total:						8,776	5,821	1,868	1,355
						14,597		3,223	

Test set (13 locations)

Location	Motorway	Direction	Speed limit [km/h]	AADT [veh/day]	ASDT [veh/day]	Total sample size (all vehicle categories)		Filtered sample size (passenger cars)	
						Right lane [veh]	Left lane [veh]	Right lane [veh]	Left lane [veh]
L2	A1	Blato na Cetini − Bisko	130	5,253	11,059	614	340	113	86
L5	A1	Donja Zdenčina − Jastrebarsko	130	20,603	34,474	550	773	79	99
L8	A1	Gospić − Gornja Ploča	120	9,255	22,581	688	443	114	82
L15	A3	Križ − Popovača	130	13,425	18,067	443	242	72	52
L18	A3	Nova Gradiška − Lužani	130	9,007	12,947	383	350	74	78
L21	A1	Zagreb − Karlovac	130	22,568	35,635	193	193	55	73
L23	A1	Zagreb − Karlovac	130	20,873	35,484	173	134	52	59
L27	A3	Slavonski Brod − Babina Greda	130	7,116	10,394	72	28	36	22
L28	A3	Babina Greda − Slavonski Brod	130	7,116	10,394	80	37	30	28
L29	A3	Zagreb − Slavonski Brod	120	10,471	14,445	95	68	31	50
L32	A1	Josipdol − Bosiljevo	130	10,864	25,072	98	27	52	21
L35	A1	Šibenik − Split	130	6,724	14,014	95	19	49	15
L38	A1	Posedarje − Šibenik	130	9,122	20,364	107	36	68	30
Total:						3,591	2,690	825	695
						6,281		1,520	
Total (Training set + Test set):						**12,367**	**8,511**	**2,693**	**2,050**
						20,878		**4,743**	

APPENDIX B – VARIABLES – DESCRIPTIVE STATISTICS

Training set (26 locations)								
Operating speed values	**Symbol**	**Unit of measure**	**Type**	**Mean**	**StDev**	**Min**	**Max**	**Median**
Operating speed (V85) – Right (driving) lane	V85R	[km/h]	Continuous	144.55	9.45	126.03	159.67	143.96
Operating speed (V85) – Left (overtaking) lane	V85L	[km/h]	Continuous	160.84	10.32	137.83	177.39	158.29
Variables	**Symbol**	**Unit of measure**	**Type**	**Mean**	**StDev**	**Min**	**Max**	**Median**
Total tunnel length in the last 20 km	TTL	[m]	Continuous	299.77	751.46	0.00	2640.00	0.00
Speed limit	SL	[km/h]	Categorical/Continuous	120.38	13.11	100.00	130.00	130.00
Lane width	LW	[m]	Categorical/Continuous	3.65	0.16	3.25	3.75	3.75
Design speed	Vp	[km/h]	Categorical/Continuous	112.31	12.75	80.00	120.00	120.00
Previous object distance	POD	[m]	Continuous	3,939.62	2,826.73	0.00	13,400.00	3,450.00
Following object distance	FOD	[m]	Continuous	4,351.92	2,935.66	500.00	12,500.00	3,100.00
Longitudinal slope	LS	[%]	Continuous	–0.30	1.76	–4.00	4.00	0.00
Terrain type	TT	[–]	Categorical	—	—	—	—	—
Terrain type—Flat	TT–F	[–]	Binary (dummy)	0.31	0.47	0.00	1.00	0.00
Terrain type—Mountainous	TT–M	[–]	Binary (dummy)	0.19	0.40	0.00	1.00	0.00
Heavy goods vehicles share (left lane)	HVS–L	[%]	Continuous	9,704.90	4,020.42	4,458.00	22,568.00	9,064.25
Heavy goods vehicles share (right lane)	HVS–R	[%]	Continuous	18,309.08	7,075.94	8,960.00	35,635.00	17,180.00
AADT	AADT	[veh/day]	Continuous	1.88	1.48	0.10	4.80	1.20
ASDT	ASDT	[veh/day]	Continuous	3.78	1.55	1.60	7.00	3.50
Traffic flow density (left lane)	TFD–L	[veh/km/lane]	Continuous	0.31	0.47	0.00	1.00	0.00
Traffic flow density (right lane)	TFD–R	[veh/km/lane]	Continuous	0.19	0.40	0.00	1.00	0.00

Test set (13 locations)

Operating speed values	**Symbol**	**Unit of measure**	**Type**	**Mean**	**StDev**	**Min**	**Max**	**Median**
Operating speed (V85) – Right (driving) lane	V85R	[km/h]	Continuous	145.07	8.62	130.78	160.90	144.28
Operating speed (V85) – Left (overtaking) lane	V85L	[km/h]	Continuous	157.44	5.38	148.43	168.95	156.82
Variables	**Symbol**	**Unit of measure**	**Type**	**Mean**	**StDev**	**Min**	**Max**	**Median**
Total tunnel length in the last 20 km	TTL	[m]	Continuous	145.38	369.83	0.00	1200.00	0.00
Speed limit	SL	[km/h]	Categorical/Continuous	128.46	3.76	120.00	130.00	130.00
Lane width	LW	[m]	Categorical/Continuous	3.71	0.09	3.50	3.75	3.75
Design speed	Vp	[km/h]	Categorical/Continuous	116.92	7.51	100.00	120.00	120.00
Previous object distance	POD	[m]	Continuous	5857.69	3488.19	1800.00	12500.00	4800.00
Following object distance	FOD	[m]	Continuous	3842.31	3506.18	0.00	13400.00	3300.00
Longitudinal slope	LS	[%]	Continuous	–0.18	2.04	–3.50	4.00	0.00
Terrain type	TT	[–]	Categorical	—	—	—	—	—
Terrain type—Flat	TT–F	[–]	Binary (dummy)	0.54	0.52	0.00	1.00	1.00
Terrain type—Mountainous	TT–M	[–]	Binary (dummy)	0.08	0.28	0.00	1.00	0.00
Heavy goods vehicles share (left lane)	HVS–L	[%]	Continuous	1.39	2.00	0.00	7.14	0.75
Heavy goods vehicles share (right lane)	HVS–R	[%]	Continuous	25.24	14.74	6.54	55.79	21.64
AADT	AADT	[veh/day]	Continuous	11722.81	5880.25	5253.00	22568.00	9255.00
ASDT	ASDT	[veh/day]	Continuous	20379.15	9613.38	10394.00	35635.00	18066.50
Traffic flow density (left lane)	TFD–L	[veh/km/lane]	Continuous	2.02	1.31	0.50	4.20	1.80
Traffic flow density (right lane)	TFD–R	[veh/km/lane]	Continuous	3.87	1.26	2.20	5.50	3.30

APPENDIX C – CORRELATION MATRIX

	V85R	V85L	HVS–L	HVS–R	TTL	SL	LW	Vp	POD	FOD	LS	TT–F	TT–M	AADT	ASDT	TFD–L	TFD–R
V85R	**1.00**	**0.85**	−0.05	0.02	−0.03	0.01	0.36	0.36	0.21	−0.27	−0.05	0.17	**−0.56**	−0.15	−0.20	−0.45	−0.49
V85L	**0.85**	**1.00**	0.03	−0.03	−0.01	−0.13	0.37	0.37	0.02	0.02	−0.02	0.09	−0.33	−0.02	−0.05	−0.35	−0.38
HVS–L	−0.05	0.03	**1.00**	0.26	−0.23	0.34	0.14	0.14	−0.13	0.39	0.15	**0.52**	−0.10	**0.72**	**0.50**	0.15	−0.01
HVS–R	0.02	−0.03	0.26	**1.00**	0.08	−0.10	−0.25	−0.25	0.08	−0.04	−0.08	0.40	−0.27	0.25	−0.14	−0.26	−0.46
TTL	−0.03	−0.01	−0.23	0.08	**1.00**	−0.25	**−0.67**	**−0.67**	−0.33	−0.31	−0.13	−0.27	0.35	−0.19	−0.29	−0.12	−0.06
SL	0.01	−0.13	0.34	−0.10	−0.25	**1.00**	0.21	0.21	0.02	0.01	0.06	0.04	−0.39	0.26	0.23	0.01	0.07
LW	0.36	0.37	0.14	−0.25	**−0.67**	0.21	**1.00**	**1.00**	0.34	0.18	0.04	0.28	−0.48	0.20	0.28	0.32	0.22
Vp	0.36	0.37	0.14	−0.25	**−0.67**	0.21	**1.00**	**1.00**	0.34	0.18	0.04	0.28	−0.48	0.20	0.28	0.32	0.22
POD	0.21	0.02	−0.13	0.08	−0.33	0.02	0.34	0.34	**1.00**	−0.38	−0.09	0.20	−0.19	−0.27	−0.34	−0.09	−0.07
FOD	−0.27	0.02	0.39	−0.04	−0.31	0.01	0.18	0.18	−0.38	**1.00**	0.29	−0.05	0.13	0.20	0.27	0.17	0.18
LS	−0.05	−0.02	0.15	−0.08	−0.13	0.06	0.04	0.04	−0.09	0.29	**1.00**	0.13	0.06	0.08	0.00	0.31	0.35
TT–F	0.17	0.09	**0.52**	0.40	−0.27	0.04	0.28	0.28	0.20	−0.05	0.13	**1.00**	−0.33	0.36	0.00	0.04	−0.20
TT–M	**−0.56**	−0.33	−0.10	−0.27	0.35	−0.39	−0.48	−0.48	−0.19	0.13	0.06	−0.33	**1.00**	−0.02	0.13	0.21	0.30
AADT	−0.15	−0.02	**0.72**	0.25	−0.19	0.26	0.20	0.20	−0.27	0.20	0.08	0.36	−0.02	**1.00**	**0.85**	0.45	0.24
ASDT	−0.20	−0.05	**0.50**	−0.14	−0.29	0.23	0.28	0.28	−0.34	0.27	0.00	0.00	0.13	**0.85**	**1.00**	**0.53**	0.42
TFD–L	−0.45	−0.35	0.15	−0.26	−0.12	0.01	0.32	0.32	−0.09	0.17	0.31	0.04	0.21	0.45	**0.53**	**1.00**	**0.89**
TFD–R	−0.49	−0.38	−0.01	−0.46	−0.06	0.07	0.22	0.22	−0.07	0.18	0.35	−0.20	0.30	0.24	0.42	**0.89**	**1.00**